Design and Development of a New Innovative Transcatheter Mitral Valve

Ghazaale Zeinaly Fashtali

A Thesis

in

The Department

of

Mechanical and Aerospace Engineering

Presented in Partial Fulfillment of the Requirements

for the Degree of Masters of Applied Science (Mechanical Engineering) at

Concordia University

Montreal, Quebec, Canada

November 2018

CONCORDIA UNIVERSITY
School of Graduate Studies

This is to certify that the thesis prepared,

By: **Ghazaale Zeinaly Fashtali**
Entitled: **"Design and Development of a New Innovative Transcatheter Mitral Valve"**

and submitted in partial fulfillment of the requirements for the degree of

Masters of Applied Science (Mechanical Engineering)

complies with the regulations of the University and meets the accepted standards with respect to originality and quality.

Signed by the final examining committee:

Dr. R. Ganesan Chair

Dr. C. B. Kiyanda Examiner

Dr. N. Bouguila Examiner

Dr. L. Kadem Supervisor

Approved by _____
Dr. Mamoum Medraj, MASc Program Director
Chair of Department or Graduate Program Director

_____
Dr. Amir Asif, Dean
Faculty of Engineering & Computer Science

Date _____

ABSTRACT

Design and Development of a New Innovative Transcatheter Mitral Valve

Mitral regurgitation is the most common valvular insufficiency, affecting more than 10% of people older than 75 years old in the United States. This translates into approximately 4 million people suffering from significant mitral regurgitation and 250,000 new cases of severe mitral regurgitation every year. The objective of this thesis is to design and test a novel transcatheter mitral valve with in-stent artificial chordae tendineae that better reproduces the native mitral complex as well as studying the cruciality of the role of chordae tendineae as a part of mitral valve apparatus.

For this purpose, numerous valves were designed and tested under physiological conditions before the optimal design was obtained. In order to study vorticity fields, viscous energy dissipation, and mitral regurgitation, the data collected from PIV measurements containing velocity fields were post processed. Particle trajectory was also performed to trace the particles inside the ventricle, during systole.

Findings of this study show that addition of the artificial chordae leads to a better performance of the mitral valve in terms of leaflet coaptations. In addition to what has been said, presence of the artificial chordae leads to significant improvements in terms of flow patterns, vortex formation, viscous energy dissipation and mitral valve regurgitation compared to the case in which the chordae were removed.

Acknowledgements

I would first like to thank my thesis advisor Dr. Lyes Kadem for introducing me to this topic and for all the continuous support, for his wisdom, motivation, patience and immense guidance. The door to Prof. Kadem office was always open whenever I ran into a trouble spot or had a question about my research or writing. He consistently allowed this thesis to be my own work, but steered me in the right direction whenever he thought I needed it.

I would also like to thank Dr. Wael Saleh who were involved in the experimenting process for this research project. Without his passionate participation and input, the experimenting process could not have been successfully conducted.

It has been a pleasure to be a member of the Laboratory of Cardiovascular Fluid Dynamics, and I am very thankful to the members of the lab for their help and assistance during my master program. Many thanks to Giuseppe Di Labbio, Amanda Mikhail, Ahmed Darwish and Nasibeh Mirvakili for helping me at different stages of the thesis. I am also thankful to all the support staff at Concordia University.

Above all, I must express my very profound gratitude to my love, Vahid, my mother Fatemeh and my father Khoshnoud for providing me with unfailing support and continuous encouragement throughout my years of study and through the process of researching and writing this thesis. My deepest appreciation goes to my brother, Saeed, who has always supported me and has always been the great joy of my life. This accomplishment would not have been possible without them.

Contents

List of Figures

List of Tables

Nomenclature

A	Anterior
AML	Anterior Mitral Leaflet
AOL	Aortic Leaflet
AS	Atrial Side
FDM	Fused Deposition Modeling
IPM	Inferior Papillary muscle
LC	Lateral Commissure
LV	Left Ventricle
MC	Medial Commissure
ML	Mitral Leaflet
MR	Mitral Regurgitation
MV	Mitral Valve
P	Posterior
PML	Posterior Mitral Leaflet
SPM	Superior Papillary Muscle
VS	Ventricular Side
3D	3-Dimensional

Chapter 1

Introduction

1.1. Circulatory of Human Body

The circulatory system, also called the cardiovascular system, is an organ system. It permits blood to circulate and transport nutrients such as amino acids and electrolytes, oxygen, carbon dioxide, hormones, and blood cells to and from the cells in the body. It also provides nourishment and helps in fighting diseases, stabilizes temperature and pH, and maintains homeostasis.

The main components of the human cardiovascular system are the heart, the blood and the blood vessels. It includes the pulmonary circulation, a closed path through the lungs where blood is oxygenated; and the systemic circulation, a closed path through the rest of the body which provides oxygenated blood (Figure 1-1). Also, the digestive system works with the circulatory system to provide the required nutrients to the body and to keep the heart pumping properly [1].

The cardiovascular system is a closed system, meaning that the blood never leaves the network of blood vessels. In contrast, oxygen and nutrients diffuse across blood vessel layers and enter interstitial fluid, which carries oxygen and nutrients to the target cells, and carbon dioxide and wastes in the opposite direction. As the heart beats, the blood is circulated through the pulmonary and systemic circuits of the body (Figure 1-2).

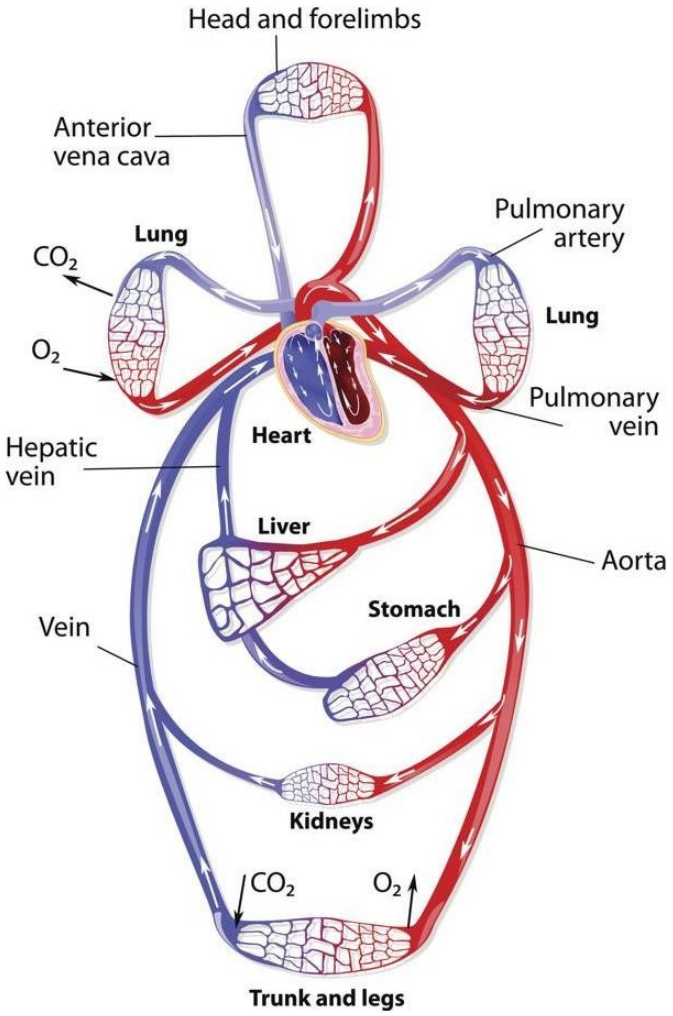

Figure 1-1. Systematic and pulmonic circulations and capillary networks [2]

There are two phases in the cardiac cycle: diastole and systole. During diastole, the ventricles are relaxed and the heart fills with blood. During systole, the ventricles contract and pump blood out of the heart to the arteries. One cardiac cycle is completed when the heart chambers fill with blood, which is then pumped out of the heart.

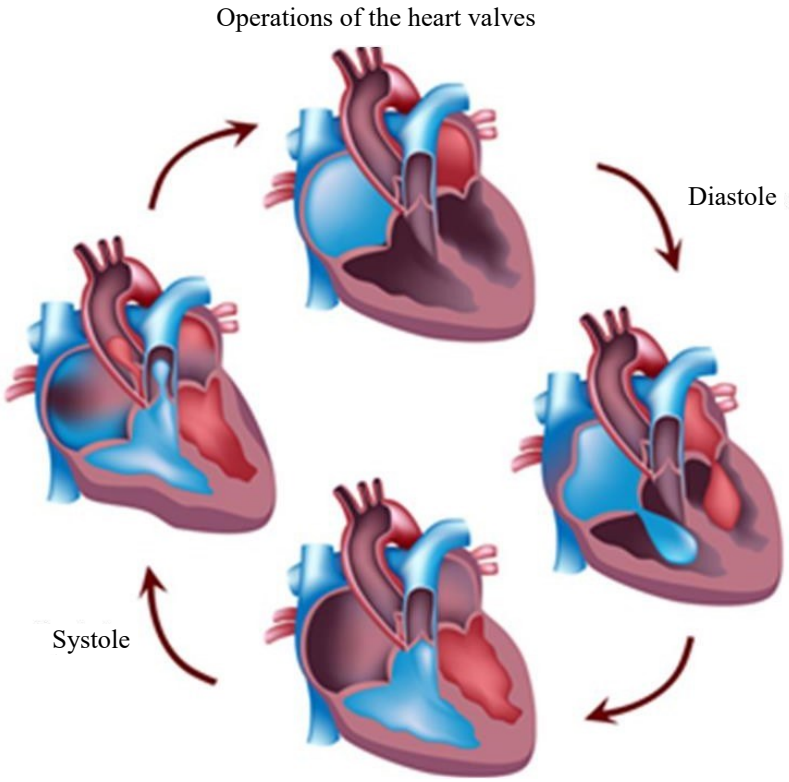

Figure *1-2***.** Systole and diastole phases of the heart [3]

1.2. Heart Valves

Heart valves allow blood flow only in the desired direction. In other words, under normal physiological conditions, heart valves act as check valves to prevent blood from flowing in the opposite direction. Heart valves remain closed until the upstream pressure is large enough to cause blood to move forward.

Four cardiac valves do the task of guiding the blood flow through the heart; the mitral valve, the aortic valve, the pulmonary valves and the tricuspid valve (Figure 1-3). The mitral valve, is the valve between the left atrium and the left ventricle. It prevents blood from flowing backward into the pulmonary veins and therefore into the lungs, even when the pressure in the left ventricle is very high [4]. The mitral valve will be the main focus of the present thesis.

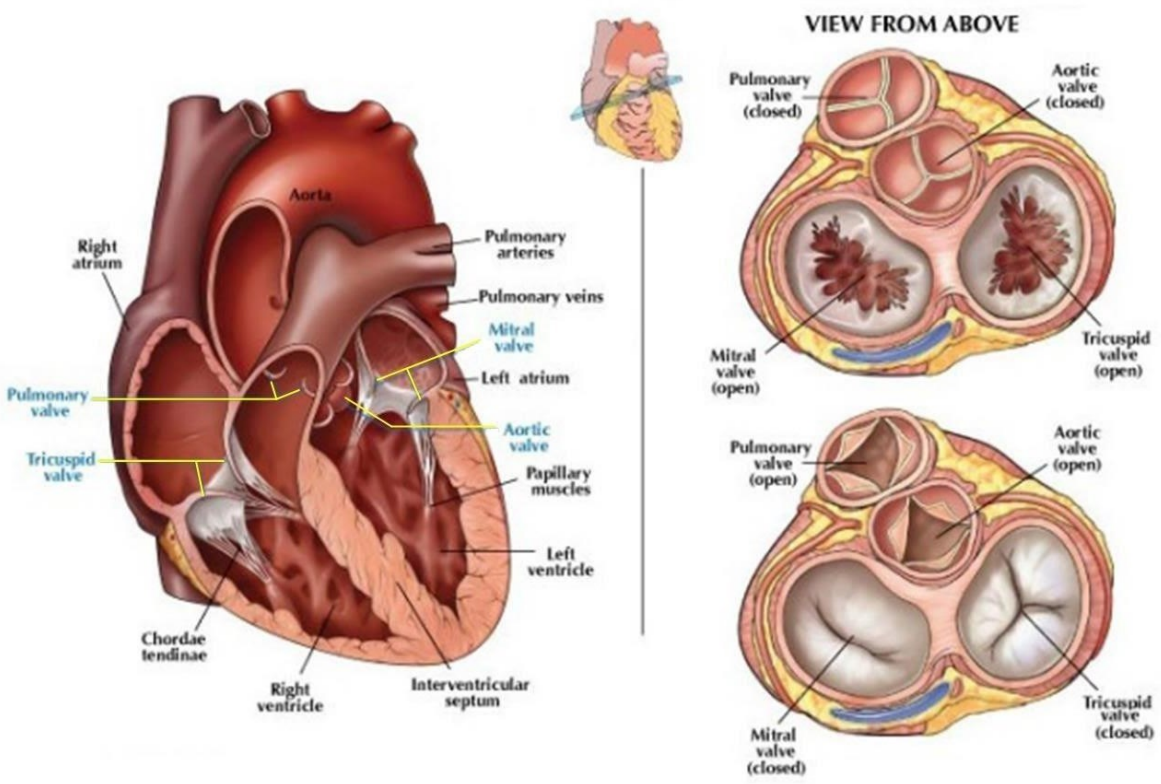

Figure 1-3. Anatomy of the heart valves [5]

1.3. Mitral Valve

The mitral valve is the passage through which the diastolic blood flow is guided from the left atrium to the left ventricle. It is also a barrier towards systolic blood backflow from the left ventricle into the left atrium. Moreover, in order to expedite the blood flow, mitral valve is part of the left ventricular outflow tract and the aortic root. This results in rapid, efficient and forceful ejection of blood into the aortic root.

The mitral valve apparatus consists of the annulus and the leaflets (the valve), the papillary muscles, and the chordae tendineae (the sub valvular apparatus) [6]. They all contribute to an optimal functioning of the mitral valve. In addition to that, the contraction and the relaxation of the left atrium play an important role in the competence of the mitral valve. As a matter of fact, it has been affirmed that atrial contraction and relaxation is one of the crucial factors that result in mitral valve closure [7]. It is also worth mentioning that although the onset of LV systole is not required for coaptation of the mitral leaflets at the end of atrial systole, it is the LV systole that

results in complete closure of the leaflets by causing the motion of the mitral leaflets towards the mitral annular plane [8].

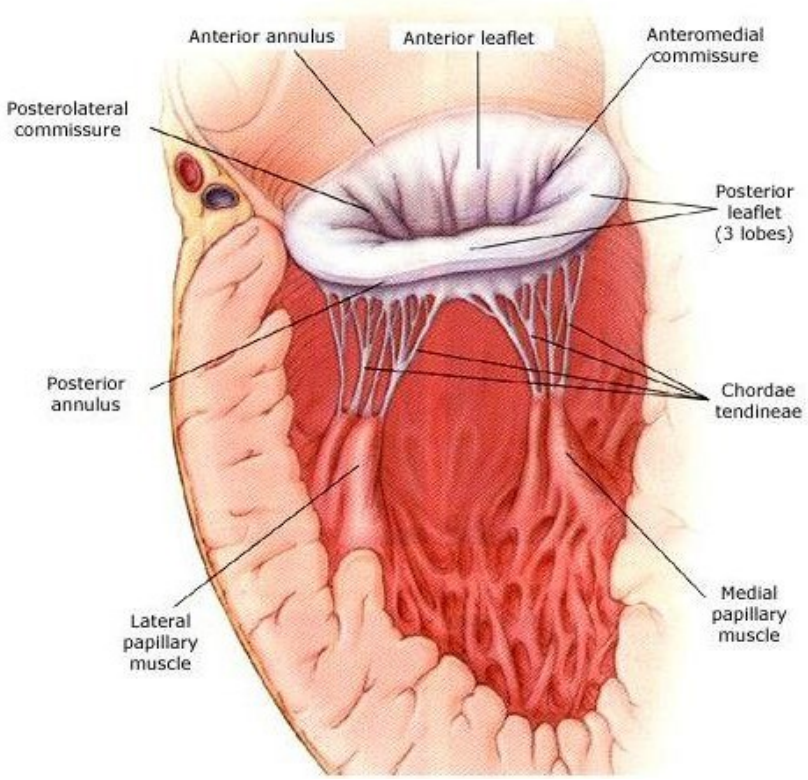

Figure 1-4. The mitral apparatus [9]

1.3.1. Leaflets

Although it is more correct to define the two leaflets of the mitral valve as antero-superior and infero-posterior, in regards to a more appropriate description of their real orientation [6], they are more commonly referred to as the anterior and posterior leaflets [10].

The two leaflets of the mitral valve are noticeably different in structure. In fact, the posterior leaflet occupies two-thirds of the circumference of the left atrioventricular junction and is relatively narrow, while the anterior leaflet is much broader and comprises one-third of the annular circumference. In adults, there are three scallops, formed by the indentations along the posterior free edge [10].

1.3.2. Annulus

In a 2D view, the mitral valve appears to own more of a D-shaped annulus than a circular one, with the inter-commissural diameter being longer than the septo-lateral one [6]. In a 3D view, it is far from being a planar structure (Figure 1-5). As a matter of fact, a distinct saddle-shaped configuration with the highest point along the anterior annulus towards the left atrium and the lowest point at the level of the commissures, the shape of a hyperbolic paraboloid, can be observed in mitral annulus anatomy [6].

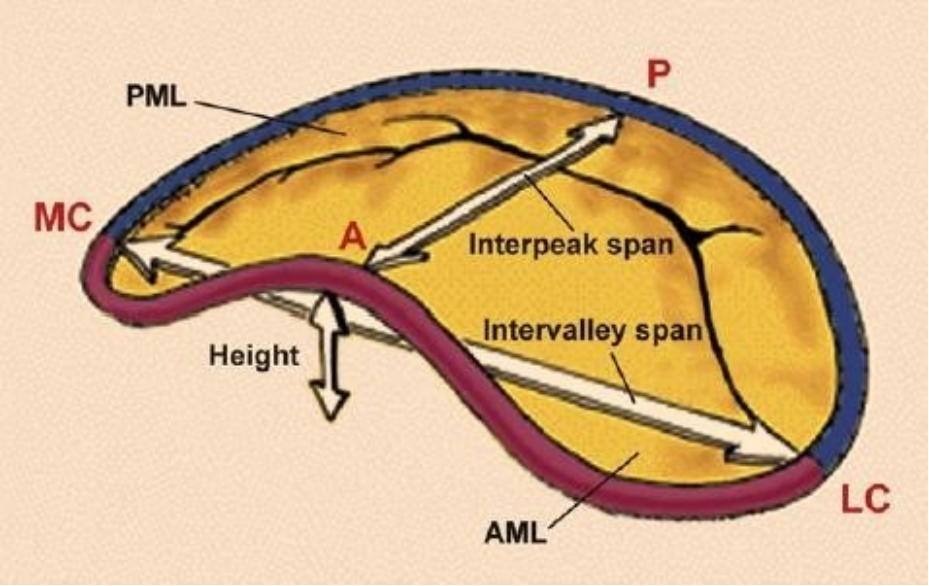

Figure 1-5. Saddle-shaped mitral annulus [11] A: Anterior, AML: Anterior Mitral Leaflet, LC: Lateral Commissure, MC: Medial Commissure, P: Posterior, PML: Posterior Mitral Leaflet

1.3.3. Papillary Muscles

In order to compensate for the geometric changes of the left ventricular wall, the mitral valve apparatus includes papillary muscles that act as shock absorbers [6]. The papillary muscle bundles are generally located in the anterolateral and posteromedial positions. Additionally, they are usually attached at the border of the anterolateral (lateral) and infero-lateral (posterior) walls. Some of them are also positioned along the mid to apical segments, over the inferior wall of the left ventricle. In the majority of adults, the papillary muscles can have up to three heads [10].

1.3.4. Chordae Tendineae

In order to form the tensor apparatus of the valve, the tendinous cords of the mitral valve relate the leaflets to either two groups of papillary muscles or to the posterior muscular wall [6]. There are different classifications of mitral chordae tendineae as summarized by Muresian [12] and can be seen in Table 1-1 and Figure 1-6.

Table 1-1. Classification of mitral valve chordae tendineae [12]

Old Terminology	**Lam et al. (1970)**	**Ritchie et al. (2005)**
First Order [a]	Commissural	Commissural
	Rough zone cords of AOL and ML that insert into the free margin	Posterior marginal cord
	Branches of the cleft cords of the ML	Anterior marginal cord
Second Order [b]	Rough zone cords of AOL and ML that insert beyond the free margin	Posterior intermediate cord
	Strut cords of the AOL	Anterior strut cord
	Main stem of cleft cords of the ML	
Third Order [c]	Basal cord of ML	Basal posterior cord
Type of cord	**Major Role**	**Equivalent Traditional Terms**
Proposed simplified classification		
Marginal cord	Essential for coaptation	"first order"
Rough zone cord	Essential for leaflet geometry	"second order"
Strut (Sustain) cord	Essential for ventricular geometry	
Basal cords	Annular reinforcement	"Third order"

[a] Inserting on the free edge of the leaflet
[b] Inserting on the ventricular aspect of the leaflet and contributing to the rough zone
[c] origin from the posterior left ventricular wall

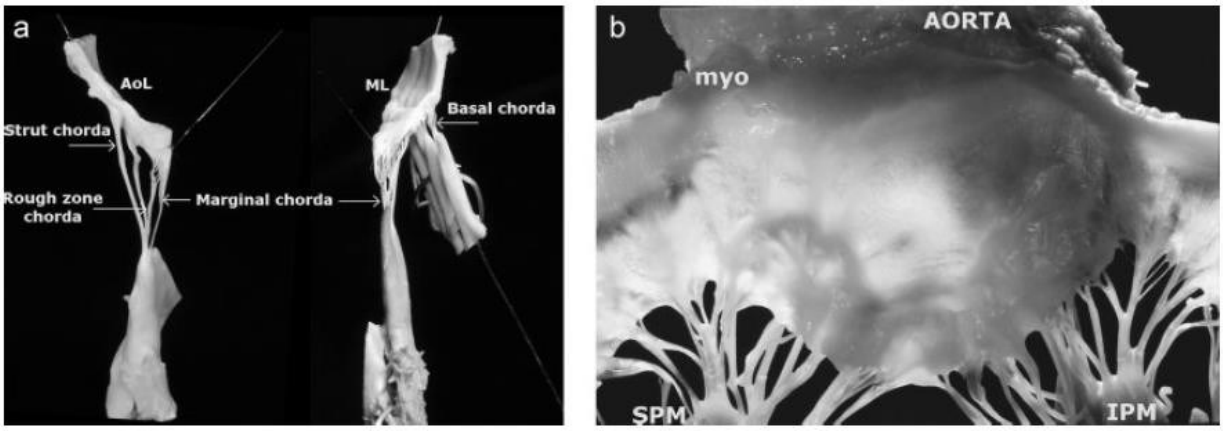

Figure 1-6. Chordae tendineae of the mitral valve [12]. AOL: Aortic Leaflet, ML: Mitral Leaflet, IPM: Inferior (posteromedial) Papillary Muscle, SPM: Superior (anterolateral) Papillary Muscle

Figure 1-6a, presents a special anatomical preparation demonstrating the locations of chordae tendineae and their connection to the two leaflets: anterior and posterior. The wider anterior leaflet allows for a better identification of the marginal cord, the rough zone cord and the strut cord. Since some of the rough zone cords intermix with the marginal cords, it is usually difficult to completely separate the two types, both functionally and anatomically. Hence, it is safe to simply say that rough zone cords are divided in two or more branches. There is also the posterior leaflet which is attached to the characteristic basal cords, originated from the ventricular wall and bas-relief shaped muscular structures. Figure 1-6b demonstrates the anterior leaflet, the adjacent commissural areas and thus the intra-leaflet distribution of the chordal support [12].

1.3.5. Posterior Left Atrial Wall

The role of atrial contraction is crucial for a correct closure of the mitral valve [6]. As a matter of fact, contractility, as a result of atrial activity rather than flow, has been considered the main determinant of mitral valve closure. One of the factors that can contribute to mitral regurgitation is left atrial enlargement. In other words, as mitral regurgitation induces left atrial enlargement, regurgitant flow may be aggravated as a consequence of the enlargement itself [7].

1.4. Mitral Valve Regurgitation

Mitral regurgitation (MR) is defined as an abnormal reversal of blood flow from the left ventricle to the left atrium (Figure 1-7). Etiology of MR can be classified as:

a) Primary mitral regurgitation

b) Secondary mitral regurgitation

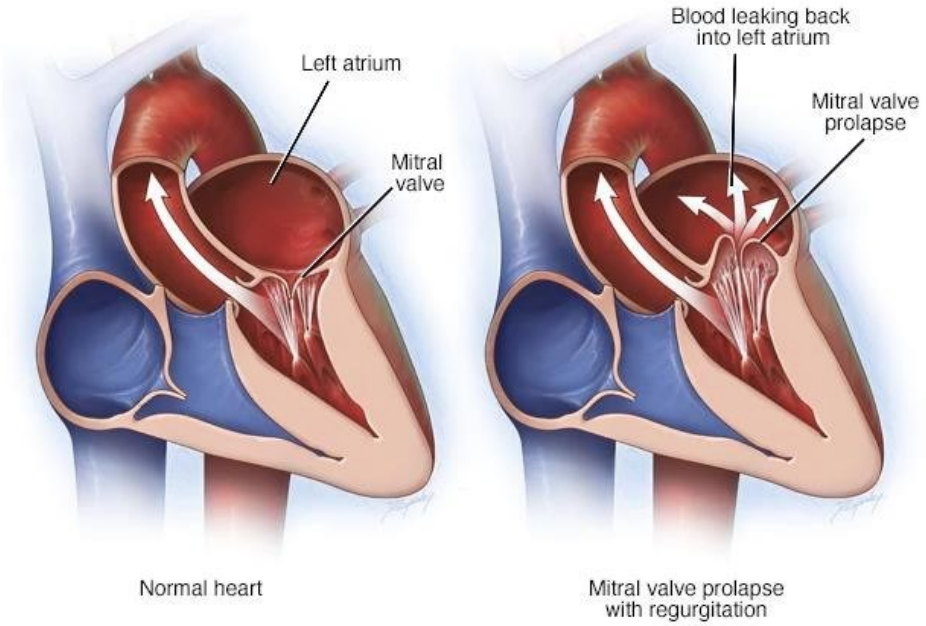

Figure 1-7. In mitral valve prolapse, the leaflets expand into the left atrium during the heart's contraction. This can lead to blood leakage into the left atrium from the ventricle, which results in mitral regurgitation [13]

Primary MR happens when biological changes in the mitral valve tissue lead to leaflets and chordae weakening and rupture. This leads to an impaired systolic leaflet coaptation (Figure 1-8).

In secondary MR, the valve tissue is normal and regurgitation happens due to the reduction and/or elimination of the normal systolic coaptation of the mitral valve leaflets [14].

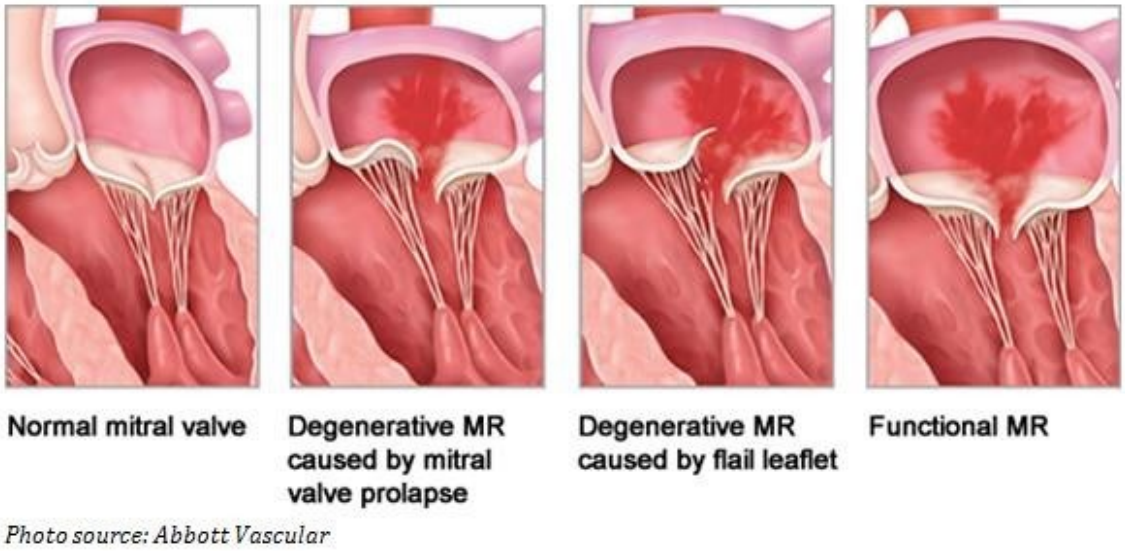

Figure 1-8. Two types of mitral regurgitation: degenerative (primary) and functional (secondary) [15]

In either case, blood flows backward into the left atrium during systole, altering ventricular pre-load and after-load. The addition of regurgitant volume to the pulmonary venous inflow elevates diastolic ventricular pressure and wall stress, inducing structural and functional deterioration of the left ventricle. Although systolic afterload is initially reduced with MR, as regurgitation into the low resistance left atrium acts as a 'pop-off' valve, the increase in ventricular radius and the reduction in ventricular wall thickness lead to the elevation of the afterload over time. Transition from a reversible compensatory phase to an irreversible decompensatory phase results in reduced inotropy and symptoms of congestive heart failure.

In case of primary MR, such a transition occurs gradually with 90% of the patients still alive at 8 years after diagnosis of MR and 50% of them surviving without any cardiac related events. While in the case of secondary MR, the transition occurs more rapidly with only 30% of the patients surviving at 5 years without a cardiac event, i.e. heart attack, or a myocardial infarction [16].

1.4.1. Complications of Mitral Regurgitation

Mitral regurgitation is the most frequent valvular pathology in the United States. Nearly 1 in 10 people, aged 75 years or older, are affected by moderate to severe MR. This means that there are approximately 4 million people suffering from significant MR, while nearly 250,000 new cases of severe MR are added to the list, per year [17]. According to the Euro Heart Survey reports (in Western Europe), ischemic cardiomyopathy is the reason for only 7.3% of the prevalence of mitral regurgitation, while rheumatic valve disease is responsible for 14.2% and degenerative valve disease for 61.3% of them. The remaining are caused by congenital lesions, endocarditis, inflammatory valve disease or other reasons [16].

A damaged mitral valve forces the heart to work harder to keep blood flowing as it should. Over time, this extra work can lead to weakening of the heart and results in congestive heart failure. In mitral regurgitation, blood can travel back towards the pulmonary system, causing pulmonary edema. Another common complication with mitral regurgitation is the development of atrial fibrillation. A leaky mitral valve can also increase pressure in the left atrium, which can eventually cause pulmonary hypertension. This can lead to heart failure on the right side of the heart [18], [19], [20], [21].

1.4.2. Management of Mitral Regurgitation

Depending on the severity of the patient's condition, the treatment of mitral valve regurgitation ranges from adopting a healthy lifestyle, as recommended by a clinician, to surgical mitral valve replacement [22].

1.4.3. Mitral Valve Repair

The techniques of mitral valve repair include annuloplasty, quadrangular resection and re-suspension of the leaflets with artificial (Gore-Tex) cords.

Annuloplasty

Annuloplasty is performed by the implantation of a device surrounding the mitral valve (Figure 1-9). The goal of mitral annuloplasty is to restore the physiological form and function of the healthy mitral valve apparatus so that the insufficiency of mitral valve would be corrected. Nowadays, there is a wide variety of annuloplasty devices that can be selected by the cardiac surgeon, which are flexible, semi-rigid, rigid, incomplete or complete, planar or saddle-shaped. Despite all the progress during the past decades, the characterization and selection of different annuloplasty devices are mostly qualitative and subjective [23].

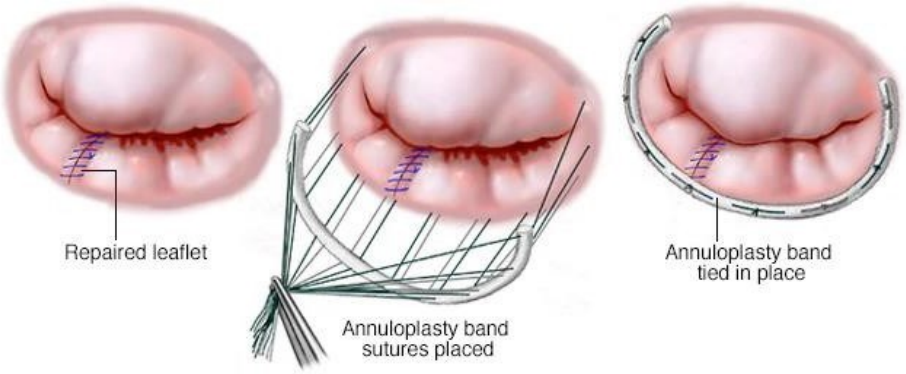

Figure 1-9. Mitral valve annuloplasty; the ring is tightened or modified around the valves in a way that the leaflets can coapt [24]

Quadrangular resection

Quadrangular resection is commonly performed in combination with either plication of the mitral annulus, sliding annuloplasty or folding plasty [25]. The quadrangular resection is accomplished by first locating the margins of the involved area where the chordae are of normal length and structure. A heavy silk tie is passed around these cords to identify and gently retract the section of the posterior leaflet that is not going to be excised (Figure 1-10). The affected or prolapsed segment is then excised. Advancement flaps are generally then created by cutting along the annulus of the remaining posterior leaflet.

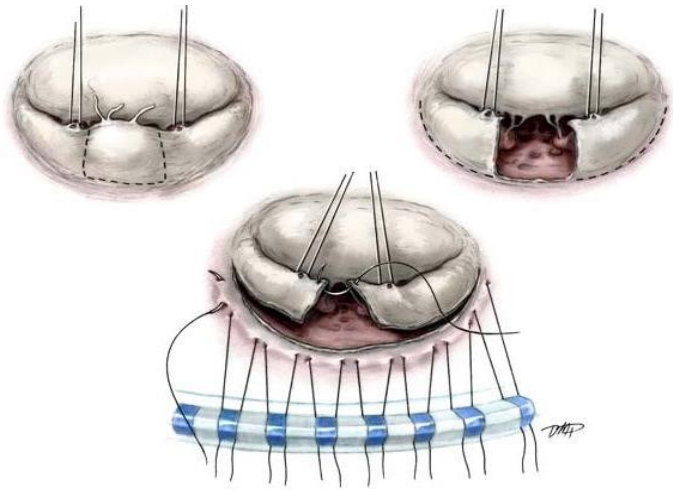

Figure 1-10. Quadrangular resection for a case with prolapse of the middle scallop of the posterior leaflet [26]

Despite the high safety and effectiveness of quadrangular resection technique and its modifications, it is worth noticing that in this method, the anatomy of mitral valve and the physiological role of the posterior leaflet is not maintained [25]. Several problems, such as left ventricular outflow tract hindrance, kicking in the circumflex artery and leaflet restriction have been reported [27]. Though widely used, this technique often leads to poor mobility of the repaired leaflet [16].

GORE-TEX Chordoplasty

Polytetrafluoroethylene (GORE-TEX) CV-5 can be used to create chordae tendineae in cases of elongated or broken cords or in circumstances in which extra cords are required to support the free edge of a leaflet after repair procedures have been performed. CV-5 sutures are used to create new cords at the central portion of the posterior leaflet [16].

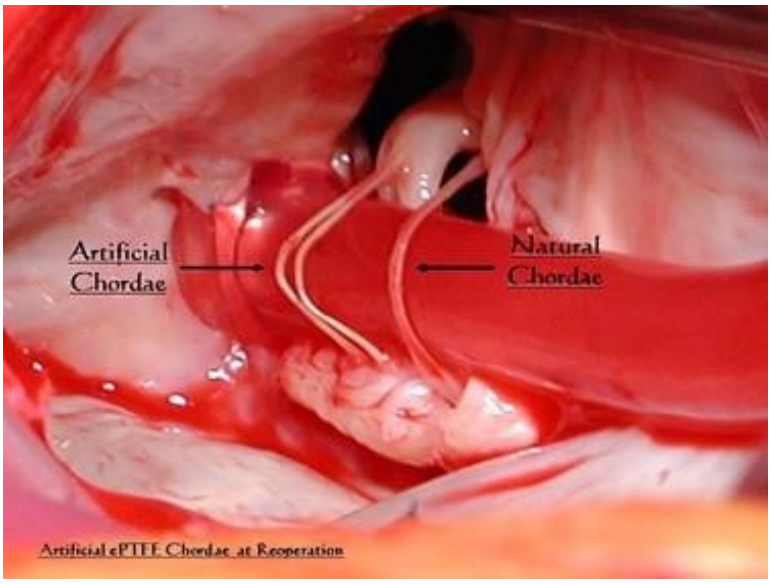

Figure 1-11. Comparison of artificial chordae tendineae and native chordae tendineae, observed after reoperation after 12 years [28]

Since secondary mitral regurgitation involves a progressively worsening ventricle and heterogeneity in the valve geometry between patients, surgical innovations in this area have had a very slow development [16].

1.4.4. Mitral Valve Replacement

Mitral valve replacement has been the recommended surgical treatment for mitral regurgitation with severe valvular insufficiency not manageable by repair, particularly in patients with severe symptomatic mitral valve regurgitation [29]. There are three primary types of artificial mitral valves: mechanical valves, tissue (biological) valves and transcatheter valves.

1.4.4.1. Surgical Replacement Procedure

In order to make the patients sleep and not susceptible to pain during the procedure, they will receive general anesthesia before the surgery. The surgeon will make a cut in the middle of the chest and will separate their breastbone so the heart could be reached. Most people are connected to a heart-lung bypass machine or a bypass pump. This machine does the work of the heart while it is stopped during the operation. A small cut is made in the left side of the heart so

the surgeon can replace the mitral valve. The mitral valve will be removed and a new one will be sewed into place. Once the new valve is working, the surgeon will close the heart and take the patient off the heart-lung machine. Then, catheters (tubes) will be placed around the heart to drain fluids that have built up. Using stainless steel wires, the surgeon will close the breastbone. It will take about 6 weeks for the bone to heal. The wires will stay inside the patient's body. A temporary pacemaker may be connected to the patient's heart until their natural heart rhythm returns. This surgery may take 3 to 6 hours [30].

1.4.4.2. Mechanical Valves

Being made from manufactured materials, mechanical valves have the main advantage of durability, since they do not wear out. However, blood tends to clot on mechanical valves, so blood thinning medication (anticoagulants) must be taken by patients for the rest of their lives. They are often implanted in younger patients so that the need for a second valve replacement procedure would be obviated. Their use also seems reasonable when anticoagulants is already being received by the patient [31].

There are three major types of mechanical valves: caged-ball, tilting disk and bileaflet valve (Figure 1-12). Bileaflet valves are the most commonly implanted.

Figure 1-12. Three major types of heart valves. Caged ball valve, tilting disk valve, and bileaflet valve respectively from left to right [32]

1.4.4.3. Tissue Valves

Glutaraldehyde-fixed tissues such as porcine valve leaflets and/or bovine pericardium are the main bioprosthetic valves. Due to their biocompatible surfaces and their improved blood flow dynamics, the risk of red blood cell damage and thrombus formation is limited in such valves. As a consequence, the need for anticoagulation is alleviated. However, as a drawback of tissue valves, durability is worth mentioning, as they last only 15–20 years, and tend to deteriorate more rapidly in younger patients. Bioprosthetic valves require replacement within 10 years in 30% of patients and within 15 years in 50% of patients [33]. Biological valvular prostheses are classified into a number of subtypes.

Homograft

A homograft, is a human heart valve that has been cryopreserved and dosed with antibiotics. Homografts are often implanted in patients with considerable evidence of endocarditis, but they are not widely available and they tend to degenerate.

Xenografts

Porcine aortic valves or bovine pericardium are used to make xenografts. They are usually fortified with a scaffolding (stent) composed of various types of materials which serves to fix the valvular tissue in its natural, anatomical-functional position (stented bioprostheses) (Figure 1-13). Preservative glutaraldehyde is frequently used to maintain the collagen scaffolding and reduce its antigenicity.

Figure 1-13. A selection of stented valvular prostheses, respectively from left to right: Hancock II, Carpentier-Edwards, Mosaic Ultra [34], [35]

According to a large-scale review, there is no difference in survival rates between patients with bioprosthetic and mechanical valves at 10 years. However, the survival rates are slightly higher at 15 years in patients with mechanical prostheses compared to the ones with bioprosthetic valves. Higher rates of degeneration and reoperation have been observed with the usage of bioprostheses [31]. It is also worth noticing that as a result of anticoagulation, hemorrhagic complications are significantly more prevalent in patients with mechanical valves.

Also, the new generation of biological prostheses have recently been of particular interest, with extended durability, a decrease in mortality when reoperating and an increase in life expectancy [31].

1.4.5. Transcatheter Mitral Valve Replacement

Beyond the challenges caused by the pathology, the risk of surgical valve repair or replacement often leads to the refusal of open heart surgery as a solution, both from cardiologists and patients. This is particularly true regarding the elderly population where mitral regurgitation is even more frequent and surgical correction of mitral regurgitation has often a high operative risk [19]. Consequently, as an efficient substitute to surgery, different percutaneous transcatheter techniques have been developed over the years [36].

The broad range of the disease that affects the mitral valve have resulted in an increased need for the development of a transcatheter mitral valve replacement (TMVR) device (Figure 1-14) [37].

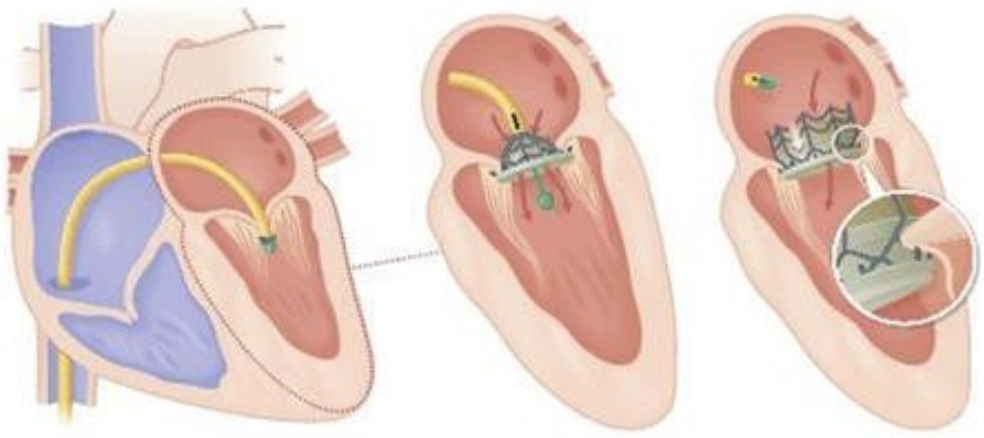

Figure 1-14. Transcatheter mitral valve replacement device [38]

1.4.5.1. TMVR Procedure and the Challenges

TMVR is performed by implanting a mitral valve using a percutaneous and non-surgical approach. In TMVR, prosthetic valve leaflets are assembled on a metallic mesh structure, called a stent, which is crimped before being introduced into the left ventricle and deployed using a balloon, or self-deploys in the instance of self-expanding valves.

As a consequence of the complexity of the mitral valve, the development of TMVR has been delayed compared to percutaneous treatments of aortic stenosis [39]. Several factors have lagged the development of a percutaneous mitral valve prosthesis:

- the asymmetry of the mitral annulus;
- absence of a single valvular plane;
- the constant movement of the mitral annulus and the basal part of the left ventricle, which challenges the stable anchoring of the prosthesis;
- the adjacency of the mitral valve to the aortic valve and left ventricle outflow tract;
- the complexity and variability of the subvalvular apparatus (chordae tendineae and papillary muscles);

- the heterogeneity of pathology and physiology of patients with mitral regurgitation (organic vs functional vs mixed disease);
- calcification of the mitral valve annulus;
- the anatomic variability of the mitral annulus [39].

1.4.5.2. Transcatheter Heart Valves

Although multiple transcatheter heart valve devices, devised to treat mitral regurgitation, are currently being developed, most of them are in early phases of evaluation with mixed technical and clinical results. A few of them are owned by larger companies and are already under evaluation in early feasibility clinical trials [40]. Here are some TMVR devices that have been implanted in humans:

- FORTIS (EDWARDS LIFESCIENCES)
- CARDIAQ-EDWARDS (EDWARDS LIFESCIENCES)
- TIARA VALVE (NEOVASC INC.)
- TENDYNE BIOPROSTHETIC MITRAL VALVE SYSTEM (TENDYNE HOLDINGS, INC.)

FORTIS Transcatheter Mitral Valve

The FORTIS valve (Edwards Lifesciences) consists of a self-expanding nitinol frame, tri-leaflet bovine pericardial tissue, an atrial flange, and opposing paddles that hook the native mitral leaflets and secure them to the frame [41].

Figure 1-15. The Fortis (Edwards Lifesciences) mitral transcatheter heart valve comprises three parts: the atrial flange, the ventricular side (or valve body), and 2 paddles (black arrows) [42]

CardiAQ-Edwards Transcatheter Mitral Valve System

The CardiAQ-Edwards transcatheter mitral valve (Edwards Lifesciences) is a self-expanding nitinol valve with a tri-leaflet bovine pericardial tissue. The attachment mechanism consists of left ventricular anchors that join the native mitral leaflets and annulus and preserve the subvalvular apparatus [41]. This is the first percutaneous valve implanted in the mitral position in a native valve [39].

Figure 1-16. CardiAQ-Edwards transcatheter mitral valve [41]

Tiara Mitral Valve System

The Tiara valve (Neovasc Inc.) consists of a nitinol self-expanding frame and tri-leaflet bovine pericardium. The valve is designed in a way that fits the D-shaped mitral annulus. The

prosthesis can be seated onto the atrial portion of the mitral annulus, getting support from its atrial portion, and the ventricular anchoring structures are designed to secure the valve into the fibrous trigones and the posterior section of the annulus [41].

Figure 1-17. Tiara transcatheter mitral valve [41]

Tendyne Bioprosthetic Mitral Valve System

A new version of the Lutter valve, the Tendyne bioprosthetic mitral valve system (Tendyne Holdings, Inc.), consists of a tri-leaflet valve of porcine pericardium, two self-expanding nitinol stents, an adjustable tether, and an apical fixation/sealing pad. The inner stent is one size and circular, and the outer stent is D-shaped to conform to the shape of the mitral annulus [41].

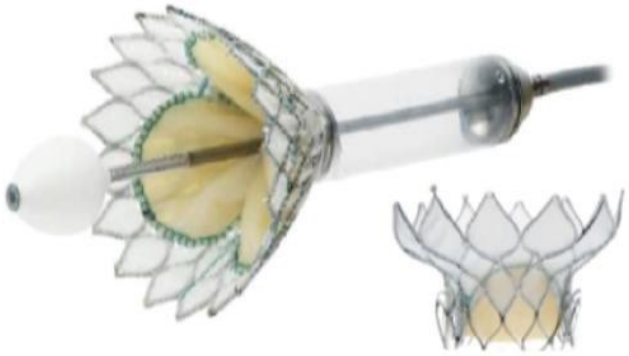

Figure 1-18. Tendyne bioprosthetic mitral valve [41]

1.4.6. Need for Alternative Valves

The currently existing products are in the trial phase. The main limitation associated with the existing products is that they do not replicate correctly the mitral valve complex. To be more specific, all the current products for TMVR include three leaflets and a circular annulus, while the native mitral valve is comprised of two asymmetric valves and its annulus is oval or D-shaped. There are also chordae tendineae in the native mitral valve via which valve leaflets are anchored to the left ventricle wall, while the current products do not have any chordae tendineae.

Hence, there is a greater need for a transcatheter mitral valve, which better reproduces the native mitral valve complex compared to existing products, as well as is better deployed in the mitral annulus. This will contribute towards the reduction in paravalvular leaks, an expected major issue for TMVR. Also, with the addition of artificial chordae tendineae, there will be a reduction in the mechanical stresses on the leaflets and consequently, an improvement in the valve durability is expected.

Chapter 2

Literature review

2.1. Introduction

Mitral regurgitation is one of the most prevalent mitral valve pathologies inducing heart failure. It can be a result of mitral valve leaflet anatomical changes or left ventricular remodeling, which may also cause the dislocation of papillary muscles. Mild and moderate mitral regurgitation usually do not require surgical interventions while severe symptomatic mitral regurgitation requires valve repair or replacement [43]. Randomized studies reveal that there is no significant difference in mortality rates between replacement and repair in ischemic related mitral regurgitation [43]. However, some medical centers are more in favor of performing mitral valve replacement rather than mitral valve repair. This is justified by the risks of poor quality of tissues, calcified annuli, and prolonged ischemic and bypass times when difficult repairs are attempted [44], [45]. Furthermore, both surgical and transcatheter valve repairs are associated with higher rates of mitral regurgitation recurrence compared to valve replacements [46].

2.2. Mechanical Mitral Valves

Being highly durable, mechanical mitral valves are one of the main choices for surgical treatment for mitral valve pathologies, particularly for younger patients. There are several companies manufacturing different types of mechanical valves, each of them having common and unique properties. Among many types of mechanical valves, Medtronic valves lead to excellent hemodynamics, in addition to its ease of implantation [33]. St. Jude Medical's mechanical mitral valve product line includes the Masters HP Series and the Regent. The original Masters Series offers a reasonable flow profile, while improving the simplicity of implantation with a controlled torque rotation mechanism and markers on the sewing cuff [33], [47]. In addition to maintaining the durability of the Masters Series with low transvalvular pressure gradients, the supra-annular

Regent provides excellent hemodynamics, even in the smallest of sizes. Sorin group produces a variety of mechanical mitral valves, called the Carbomedics line, which have been proven to have a low rate of thromboembolism in retrospective analysis of patients, compared to the other brands of mechanical valves [33].

Regardless of the type of the mechanical valve, severe side effects such as an increased risk of hemorrhagic stroke and gastrointestinal bleeding, because of the lifelong anticoagulation therapy (i.e., warfarin), still exist. These side effects lead to a limitation of the patient's ability to participate in certain activities and even result in a mortality of 1% of patients per year [33], [48]. In order to prevent blood coagulation, providing a surface that prevents platelet adhesion can be a solution for the future. In fact, improvements in surface coatings on valves can contribute to a reduction in platelet activation, thrombus formation, and protein aggregation. In a particular technique, scientists apply horseradish peroxidase (HRP) as a catalyst, through a polymerization process, to make hydrophilic polymers required to create a non-adhesive outer coating [48].

In a study performed on four of the most commonly implanted mechanical valves, St. Jude Medical, the CarboMedics, the Duromedics and the Sorin Bicarbon valve, some obstruction of blood flow was observed even when they functioned normally. In fact, the mean pressure gradient of all four prostheses exceeded the normal values and the pressure half-time derived since the effective mitral valve area is smaller compared to the native mitral valves [49].

2.3. Bioprosthetic Mitral Valves

The biocompatible surface of bioprosthetic valves and improved blood flow dynamics are the reasons for minimized red blood cell damage, reduced thrombus formation and therefore alleviated the need for anticoagulation. Although durability is a concern for these valves, improvements in stent design techniques and fixative methods can result in improvements in bioprosthetic valves' durability. Presently, the existing valves last only 15–20 years, and tend to deteriorate even more rapidly in younger patients [33].

Edwards Lifesciences offers a frequently implanted variety of pericardial heart valves for the mitral position. The Carpentier-Edwards PERIMOUNT^{TM} line, which was Edwards's second-generation bovine pericardial valve, shows notable durability compared to the first generation

pericardial valves and as a result, there is a remarkably low rate of reoperation due to structural valve deterioration in elderly patients [50]. There are also xenograft porcine valves e.g., The Duraflex^{TM} and standard mitral porcine valves, which are treated with Edwards' patented XenoLogiX treatment and located on a flexible stent, which have characteristics such as excellent hemodynamics and low rates of calcification [33], [51]. The Hancock II, Mosaic and Mosaic Ultra are the two bioprosthetic valve lines offered by Medtronic. Both of them are porcine valves, with remarkable durability and hemodynamics. The former line presents an overall low amount of valve related complications while the latter comprises a flexible stent to reduce tissue stress [33], [52]. St. Jude Medical applies porcine leaflets to produce Biocor stented valve systems and the Epic^{TM} stented valves with Linx^{TM} AC technology, which was shown to have excellent durability, even in young patients [33].

2.4. Transcatheter Mitral Valves

Notably, surgical treatments are associated with higher rates of survival. Observations indicate mortality rates of 1% to 5% and morbidity rates of 10% to 20%, including stroke, reoperation, renal failure, and prolonged ventilation, particularly in patients with left ventricular dysfunction. Those rates are even higher in elderly population with 17% mortality and 33% morbidity rates. In addition, surgery on the elderly is also associated with a high rate (>20%) of rehospitalization. For patients with secondary mitral regurgitation, survival rates with or without surgery are lower compared to the patients with a primary cause [46]. Furthermore, only a small portion of patients suffering from secondary mitral regurgitation and almost half of those suffering from primary mitral regurgitation undergo surgery. The reason behind this is that in elderly patients, surgical interventions lead to complications such as diabetes, pulmonary disease, perioperative hemodialysis and low ejection fraction, which result in a remarkable increase in the risk of operative mortality [43]. Moreover, due to the need for reoperation because of reappearance of mitral regurgitation, particularly in moderately severe or severe cases (>30%) and in patients with ischemic mitral regurgitation, a less invasive and thus less morbid approach to mitral regurgitation would be better-received [46].

The FORTIS^{TM} transcatheter mitral valve (Edwards Lifesciences Corp, Irvine, CA) presents a cloth-covered self-expanding frame with leaflets made from bovine pericardial tissue

and is designed with the purpose of minimizing paravalvular leaks. The long-term outcome from the FORTIS^{TM} valve is not yet available. Medtronic has also revealed the completion of animal studies and the progress in chronic studies using a competing product [33]. Another valve undergoing evaluation is the Tiara^{TM} mitral valve device (Neovasc, Vancouver, Canada) which is reported to have passed successful pre-clinical evaluations [53].

2.5. Challenges of Transcatheter Mitral Valves

Implantation of transcatheter mitral prostheses in native valves has proven more challenging than either aortic implants or valve-in-valve mitral implants [46]. The most significant challenges include, the necessity of a prosthesis that is larger than most aortic devices, displacement of native mitral valve leaflet tissue, the fixation of the prosthesis to a diseased mitral apparatus with greater valve complexity, the variable size of the mitral annulus, the lack of calcium, the potential need for orientation, and the noncircular annular shape. In addition to these anatomical challenges, there are also some functional challenges such as the necessity to maintain stability while ensuring cyclical native annulus movement and the requirement for valve proficiency under so many different hemodynamic flow rates and pressures [46], [33]. A decrease in survival rates after transcatheter aortic valve replacement is already proven as a result of paravalvular leaks. This will lead to even fewer survivals in the mitral valve patients with LV dysfunction which, with the higher driving pressures, may experience more frequent hemolysis. Finally, the need to preserve the subvalvular apparatus and the concern of not disturbing the LV outflow tract pose additional challenges [46].

2.5.1. Paravalvular Leaks

Among the possible complications of valve replacement, prosthetic valve paravalvular leak (PVL) is rather frequent, with a prevalence of up to 18% in surgical aortic valve replacements, 50% to 85% in transcatheter aortic valve replacements, and up to 23% in surgical mitral valve replacements. In patients with significant mitral valve PVL, symptoms of heart failure, elevated filling pressures, or hemolytic anemia are typically observed [54]. Among the risk factors for the development of paravalvular leaks, poor surgical techniques, annular calcification, and endocarditis are additional risks worth mentioning. Depending on the factors such as the surgical

findings related to the etiology, the condition of the native mitral annulus, the location and size of the leak, and the surgical exposure, the option of surgery involves either the repair of the leak or the re-replacement of the valve.With either choice, failure rates could be as high as 35% [55].

In order to avoid paravalvular leaks and valve embolization, moderate valve oversizing (5-20% in area) is recommended. However, there are few reports concerning the impact of oversizing on valve leaflet mechanical stress, i.e. increased leaflet bending stress during valve opening and closing, which can lead to a decrease in the valve's long-term durability [56]. Oversizing can also increase the risk of annulus ruptures and valve dissection, particularly in the presence of subvalvular calcium [57].

2.6. Hemodynamics

2.6.1. Mitral Vortex Ring

According to the early observations of healthy hearts, the opening of the mitral valve during the E-wave is correlated with the development of a vortex ring. This vortex ring, which occupies the entire ventricle, stores the kinetic energy of the blood and smoothly directs the blood to the outflow tract [58], [59]. Major aspects of cardiac function are reflected uniquely in the optimization of vortex formation in the blood flow during early diastole [60].

Vortices are created as a result of the separation of a fluid's boundary layer due to a sharp edge. In the left ventricle, the tips of the mitral valve leaflets are where the laminar inflow is transformed into a vortex. This vortex formation results in the smooth redirection of the blood flow toward the outflow tract during systole while creating minimal turbulence and avoiding large losses of kinetic energy [59].

Energy loss in a vortex is a consequence of the fluid's viscosity. Rapid changes in vorticity (high pulsatility), as well as interactions between many small vortices (turbulence), lead to high energy losses. That is to say, in contrast to the case in which the bloodstream splits into smaller, rapidly changing vortices, a single large and steady vortex is an energetically favorable condition. In the former situation, kinetic energy gets lost, which needs to be compensated for by the ventricular musculature [59].

Other than momentum preservation, efficient vortex formation facilitates normal leaflet coaptation at mid-diastole [61]. The presence of the intraventricular vortex is crucial to the overall synchronicity of the beating heart. The intraventricular circulation is a consequence of the asymmetry of the mitral orifice with respect to the ventricular chamber, where the eccentric inflow generates an asymmetric rotatory motion. Alterations of the mitral valve geometry, as a result of valvular diseases or implants of prosthetic valves, can have a negative impact on the cardiac vorticity [62].

2.6.1.1. Flow Pattern in Healthy Hearts

According to the idealized left ventricle models, the formation of the mitral vortex ring is highly dependent on the location of the mitral annulus, and mitral eccentricity. Diastolic flow patterns in the left ventricle are in association with the asymmetry and dynamic deformation of the left ventricle and the precise location of the effective mitral orifice, while the dynamics of the leaflets are regulated by chordae tendineae [58], [63]. Observations also show that a sufficient valve closure without regurgitation will not happen unless in the presence of an adverse pressure gradient, which decelerates the flow through the valve and moves the leaflets toward closure simultaneously [64].

During a study performed by Faludi et al., 19 patients were examined of which nine were healthy volunteers without signs or symptoms of heart disease, while ten patients had prosthetic mitral valves. Observations on all of the healthy subjects report the formation of a vortex separating from the anterior leaflet early after the peak of the E-wave, which occupies the entire left ventricle by the end of the E-wave. With atrial contractions, a second smaller vortex with the same rotational direction is generated at the very end of the diastole. Once only a single large vortex is present, the laminar blood flow is smoothly redirected toward the outflow tract in preparation for the following systole. It should be noted that because of the asymmetry of the left ventricular inflow tract, the anteroseptal side of the vortex formation dominates and persists in the center of the cavity while the smaller posterior part of the vortex disappears [59].

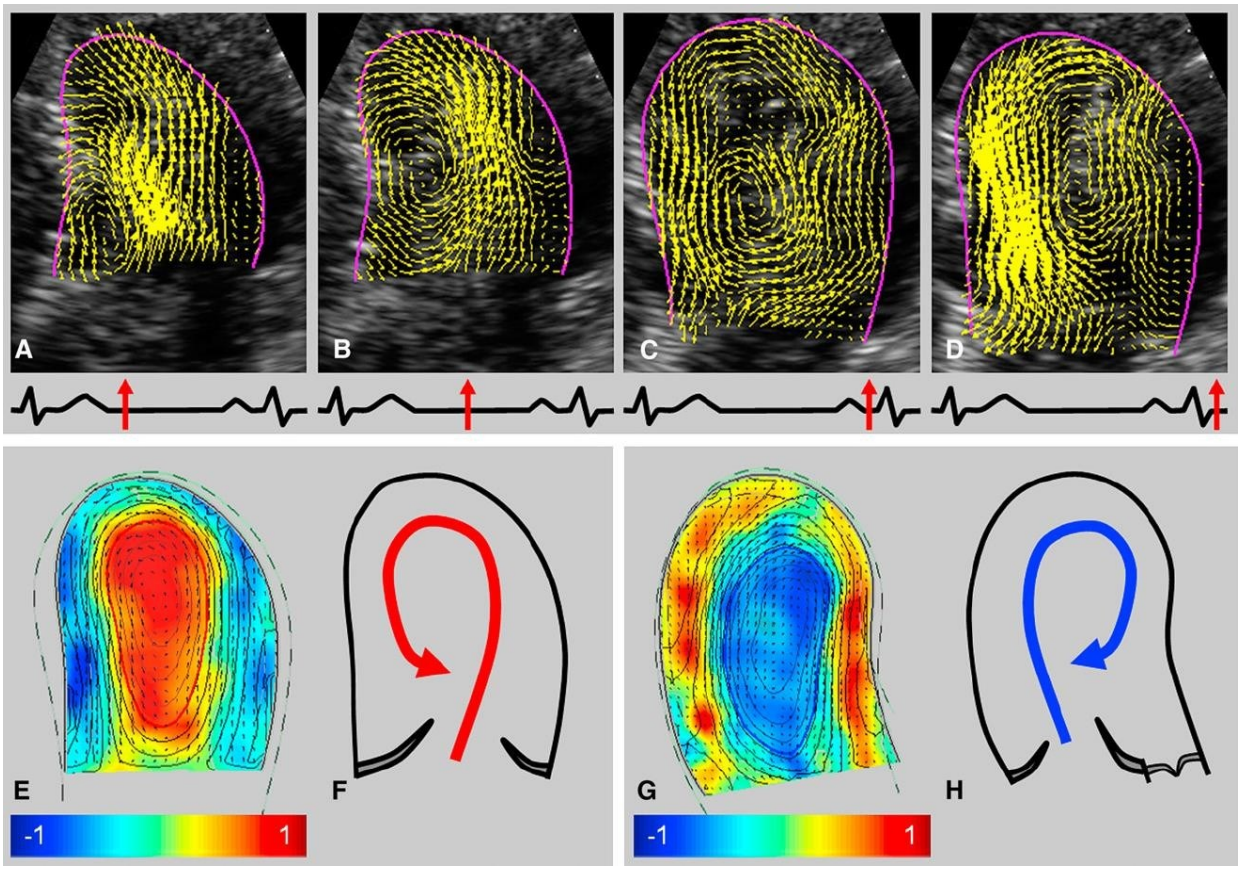

Figure 2-1. Flow pattern in a healthy left ventricle, in the presence of the native mitral valve. Yellow arrows indicate the instantaneous local direction and velocity of blood flow are superimposed [59]

2.6.1.2. Flow Pattern in Bioprosthetic (Trileaflet) Valve

The mitral plane, being deflected ~15 degrees, is not horizontal and points towards the left ventricle center. Consequently, the mitral jet enters the left ventricle directed downwards, while being parallel to the left ventricular axis, with minimal deviations. Replacing the native valve by a prosthetic one leads to the loss of the natural leaflets' asymmetry, hence disturbing the natural direction of the mitral jet and its inclination toward the ventricle center [62]. In the study performed by Faludi et al., it was observed that the flow through the bioprosthesis valves (Carpentier–Edwards; Edwards Lifesciences, Irvine, Calif) develops a central jet directed toward the apex. It develops a vortex ring that is featured as a vortex pair in a 2-dimensional image and, with atrial contraction, the same flow pattern is amplified. More precisely, in patients with bioprosthetic valves, a completely symmetric inflow pattern leads to a symmetric vortex ring. At the end of

diastole, the symmetry of the flow pattern disappears, the posterolateral vortex part dominates, and the outflowing blood crosses the previous inflow area again [59].

Finally, a noticeable increase of energy loss of about 30% with instantaneous peaks is reported, which exceeds 50% during flow deceleration during the deformation and dissipation of the vortex [62]. This could be explained by the division of the blood stream in counter-rotating parts which leads to a higher loss of kinetic energy compared to the single vortex of a normal heart [59]. As a further consequence, the distribution of pressure along the ventricle wall is completely changed. Pressure values augment in magnitude and move from the lateral to the septal wall. As a result, the normal equilibrium that developed along the boundary between pressure, tissue curvature, and stiffness is altered and some regions are subjected to stresses larger than those they were physiologically adapted to. Actually, one of the common drawbacks found in the follow-ups after mitral valve replacements, is the reshaping of the ventricular chamber. However, this fact can also be attributed to other factors such as the cutting of the chordae tendineae connecting the valve to the papillary muscles [62].

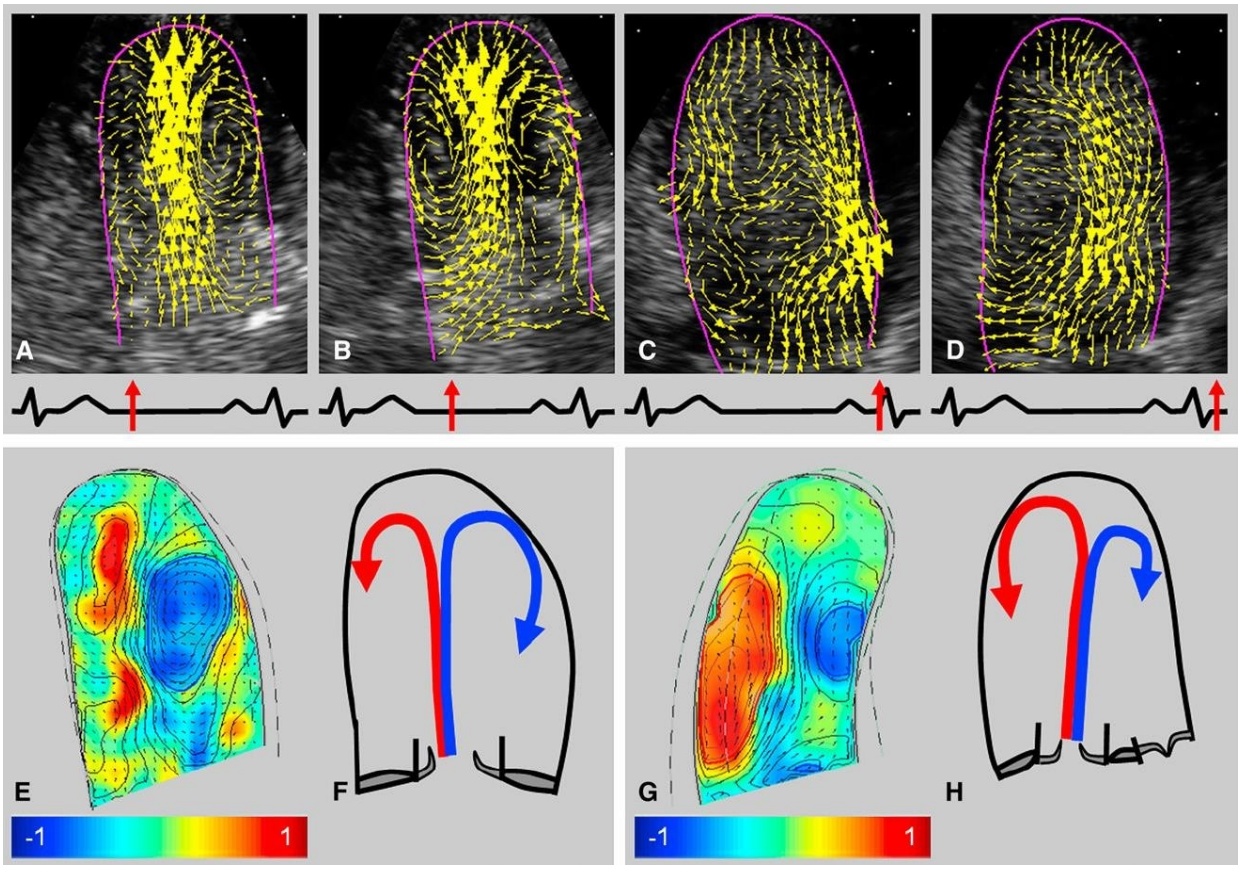

Figure 2-2. General flow pattern in patients with bioprosthetic (Trileaflet) valves [59]

2.7. Summary and Objectives

Mitral regurgitation is one of the most prevalent mitral valve pathologies inducing heart failure and, in the case of high severity, mitral valve replacement can be the best solution. For this purpose, different types of prosthetic valves are available. Although mechanical valves are highly durable compared to the other types of prosthetic valves, severe side effects result after implanting theses valves, which can include an increased risk of hemorrhagic stroke and gastrointestinal bleeding due to the lifelong anticoagulation therapy. Bioprosthetic mitral valves on the other hand, minimize red blood cell damage, reduce thrombus formation and, hence, alleviate the need for anticoagulation. However, durability is a concern for these valves.

Despite all the advantages of surgical treatments, observations indicate mortality rates of 17% and morbidity rates of 33% in the elderly population. Above all, only a small portion of patients suffering from secondary mitral regurgitation and almost 50% of those suffering from

primary mitral regurgitation undergo surgery, due to its possible complications. This is particularly true for the elderly population which could experience diabetes or pulmonary disease. As a result, a less invasive and thus less morbid approach to mitral regurgitation would be better-received. However, there are several challenges on the way.

Prosthetic valve paravalvular leak is one of the most frequent challenges of valve replacement. Depending on factors such as the condition of the native mitral annulus, the location and size of the leak, the option of surgery involves either the repair of the leak or the re-replacement of the valve. With either of those choices, failure rates could be as high as 35%. In order to avoid paravalvular leaks, moderate valve oversizing (5-20% in area) is recommended. However, there are reports indicating the impacts of oversizing such as increase in leaflet bending stress during valve opening and closing, which can lead to a decrease in the valve's long-term durability. Oversizing can also increase the risk of annulus ruptures and valve dissection.

The other challenge regarding mitral valve replacement is the undesirable changes in the blood flow patterns. In healthy hearts, diastolic flow patterns in the left ventricle are in association with the asymmetry and dynamic deformation of the left ventricle and the precise location of the effective mitral orifice, while the dynamics of the leaflets are regulated by chordae tendineae. Replacing the native valve by a prosthetic one, which comprises three leaflets located on a planar surface and lacks chordae tendineae, leads to the loss of the natural leaflets' asymmetry, hence altering the direction of the mitral jet, which results in an altered flow pattern. Specifically speaking, deviating from the anatomy of the native mitral valve, leads to alterations in mitral vortex ring formation. Major aspects of cardiac function are reflected uniquely in the optimization of vortex formation in the blood flow during early diastole.

The objective of this thesis is to promote healthy-like flow patterns in a heart with an artificial transcatheter implanted mitral valve. Healthy flow patterns will lead to reduced occurrence of complications such as heart failure. To this end, we investigate the flow patterns resulting by passage through a novel transcatheter mitral valve with in-stent artificial chordae tendineae, designed and tested to better reproduces the native mitral complex as well as to study the cruciality of the role of chordae tendineae as a part of mitral valve apparatus.

Chapter 3

Methodology

This chapter gives a detailed description of the experimental system and procedures used for data acquisition throughout the experiment.

3.1. Left Ventricle

3.1.1. 3D printed models

For the purpose of having the most realistic left heart models possible, CT images from patients were used. However, considering the feasibility of the designed experiments, some simplifications were applied such as a symmetric left heart, an initial circular shape for the mitral annulus. After converting the files to a STL format, they were 3D printed using PLA filament and sanded to improve surface smoothness and optimize silicone coating. Table 3-1 presents some of the properties of PLA filament.

Table 3-1. Properties of PLA filament [65]

Tensile Strength	37 MPa
Elongation	6%
Flexural Modulus	4 GPa
Density	1.3 g/cm^3
Melting Point	137 ℃
Biodegradable	Yes, under the correct conditions
Glass Transition Temperature	60 ℃

3.1.2. Elastic models

In order to closely mimic a real heart during the ventricular contraction and expansion, silicone was considered as the material for the elastic models. In that regard, a mixture of silicone (Polycraft T-4 Translucent Silicone Rubber) and the curing agent, with a mixture ratio of 10:1 by weight was used. Table 3-2 presents some properties of the silicone used. As the fabricated ventricle was supposed to be used for optical velocity measurements using particle image velocimetry, one of the crucial considerations in the fabrication process was the absence of air bubbles in the surfaces. For this purpose, the silicone mixture was placed in a vacuum pump (VacuTec, 800EV2), for about 30 minutes, so the air bubbles due to the mixing process would be removed. It took us an average of 4 evenly-coated layers to reach the desired thickness that led to a proper response to contraction and expansion forces induced by the cardiac simulator, all the while not collapsing. As expected, increasing the number of layers resulted in a higher stiffness and thus, a lower ventricular compliance. The rest time for each layer, was about 45 minutes. During the rest time, the ventricle mold was bolted in a rotating machine with a speed of 10 rpm, by which any unevenness in the surface of the ventricle would be limited. In order to shorten the curing time, the rotating machine was equipped with a heater. In addition to the four outside layers, another layer of silicone was coated on the inside surface of the ventricle in order to improve left ventricle transparency. Figure 3-1 presents pictures of the left ventricle 3D printed model, before and after taking off the silicone.

Table 3-2. Silicon properties [66]

Property	Unit	Value
Base		
Viscosity	cP	70,000
Specific gravity		1.1
XIAMETER curing Agents RTV-4234-T4 or RTV-4234-T4 O		
Viscosity	cP	300
Specific gravity		0.96
Base and curing agent mixture (100:10 by weight)		
Mixed viscosity	cP	35,000
Color		Translucent
Working time at 23℃ (73.4F)	minutes	90
Curing time	hours	12
Linear shrinkage	%	< 0.1
Cured for 24 hours at 23 23℃ (73.4F) with XIAMETER RTV-4234-T4 curing agent		
Hardness (Shore A)		40
Tensile Strength	psi	971
Tensile Strength	MPa	6.7
Elongation at break	%	400
Tear strength, Die B	ppi	150
Tear strength[1]	N/mm	27
Cured for 24 hours at 23 23℃ (73.4F) with XIAMETER RTV-4234-T4 O curing agent		
Hardness (Shore A)		40
Tensile Strength	psi	942
Tensile Strength	MPa	6.5
Elongation at break	%	375
Tear strength, Die B	ppi	180
Tear strength[1]	N/mm	32

[1] ISO 34 Cutter (equivalent JIS K 6252, DIN 53515/angle nick 1.00mm)

Figure 3-1. Left ventricle mold before and after taking off the silicone

3.2. Mitral Valve

In order to have a prosthetic mitral valve that can mimic the native one, we needed to design and fabricate the three main parts of the mitral apparatus; leaflets, annulus and chordae tendineae.

3.2.1. Annulus

For the purpose of holding the leaflets and also the artificial chordae tendineae, a stent with an oval/D-shaped cross-section was designed using SolidWorks 2017. Originally, the major and the minor diameters of the stent were 34.86 mm and 28.78 mm, respectively. This is in the size range of an adult native mitral valve. Later, due to the circular shape of the mitral annulus in our double pulse heart simulator and in order to avoid overstressing the stent and leaflet coaptation problems, we modified the diameters to 31.06 mm and 25.93 mm. This way, the original shape of the cross section would be preserved and the valve major diameter would fit the circular annulus diameter. Regarding the stent, the thickness of the struts was 0.5 mm, the depth of the stent was 2 mm and its height was 25 mm (Fig. 3-2, 3-3). After the design was completed, the stent was printed on a Lulzbot Taz 6 3D printer, with a PLA filament. The reason behind the choice of a PLA

filament was to fabricate a stent that was not flexible so that it could absorb some of the force induced by the pulsatile contractions of the ventricle and therefore, would not bend when the artificial chordae tendineae are inserted.

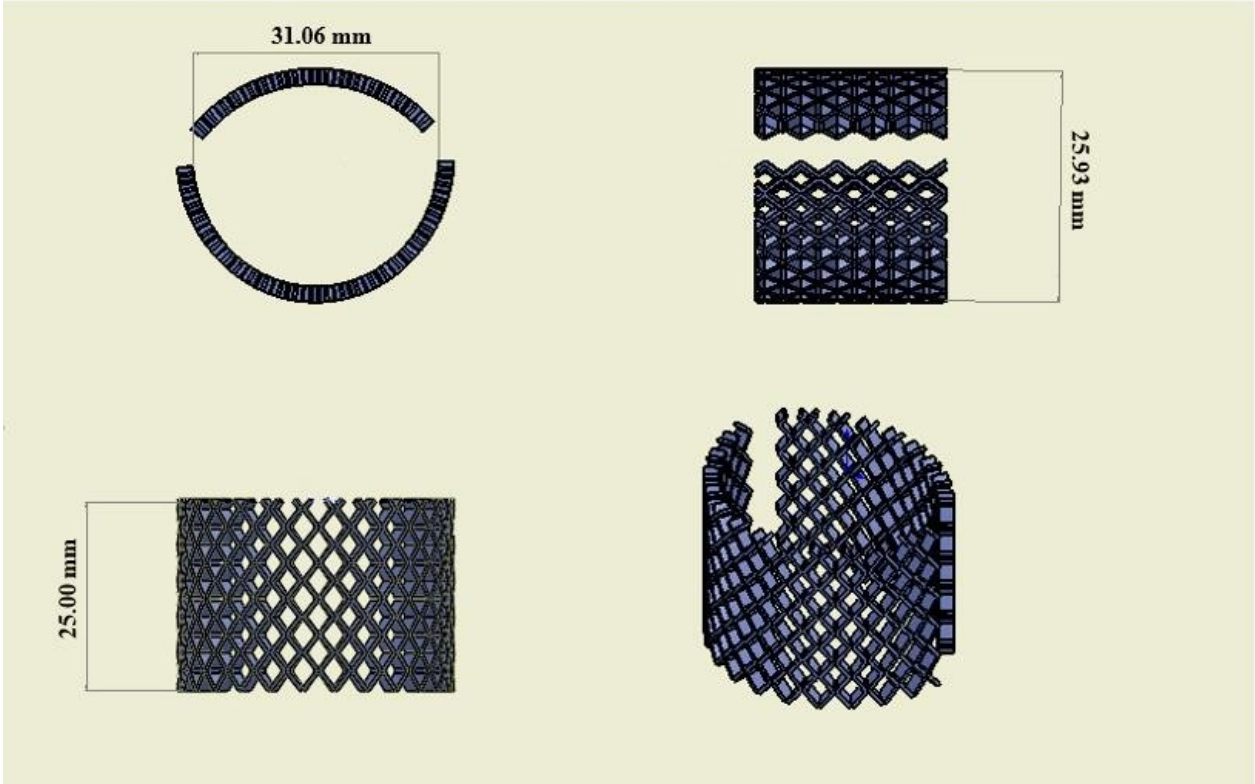

Figure 3-2. The CAD design of the stent.

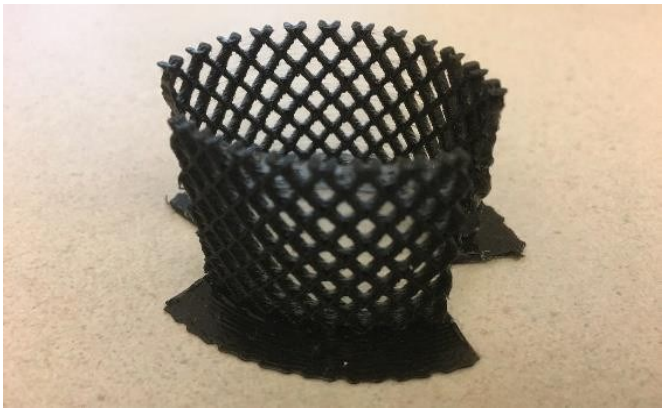

Figure 3-3. The 3D printed stent, printed by a FDM printer, Lulzbot Taz 6, with a PLA filament

3.2.2. Leaflets

The very first step in fabricating the mitral leaflets was to design a mold that would fit the inner diameters of the oval/D-shape cross section of the stent and that will be consistent with the anatomy of native mitral leaflets i.e. the asymmetry of the posterior and anterior leaflets and the curved structure of the leaflets and their dimensions (Figure 3-4). The desired mold was designed, by applying 3D sketching methods in SolidWorks 2017. It was then 3D-printed using PLA as filament.

In order to make the leaflets visually accessible while working in the cardiovascular simulator, they were made using the same mixture of silicone and curing agent as for the left ventricle. For the sake of avoiding excessive stiffening of the leaflets, only two layers of silicone were coated on the mold of the mitral valve.

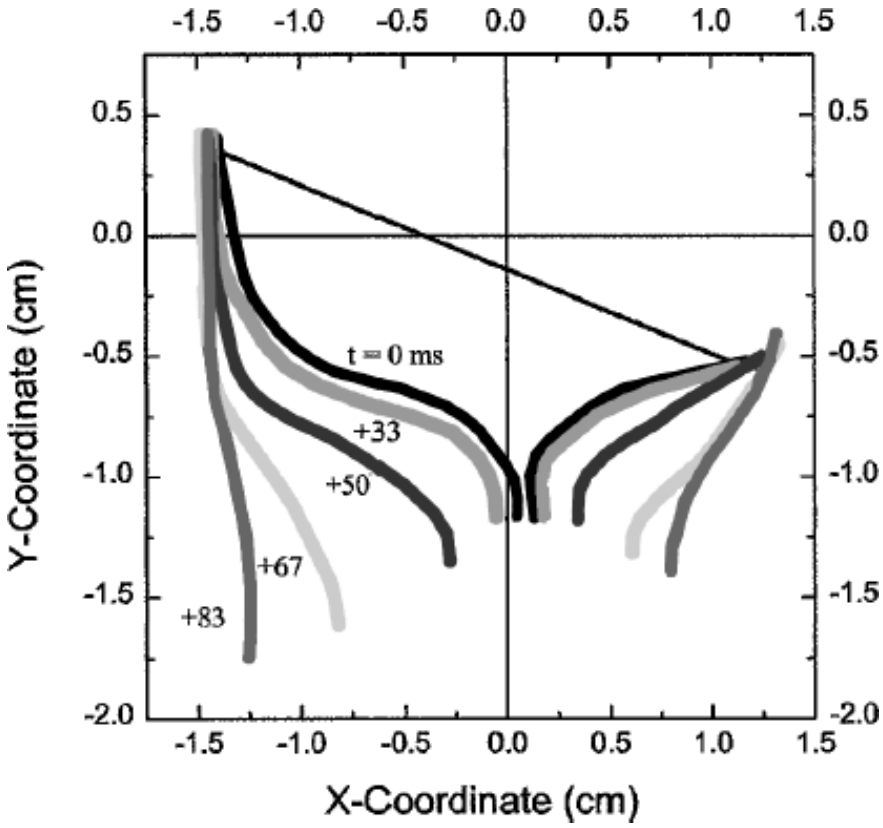

Figure 3-4. Approximation of anterior and posterior mitral valve leaflets during opening (from t = 0 to t = 183 ms) in x-y plane [67].

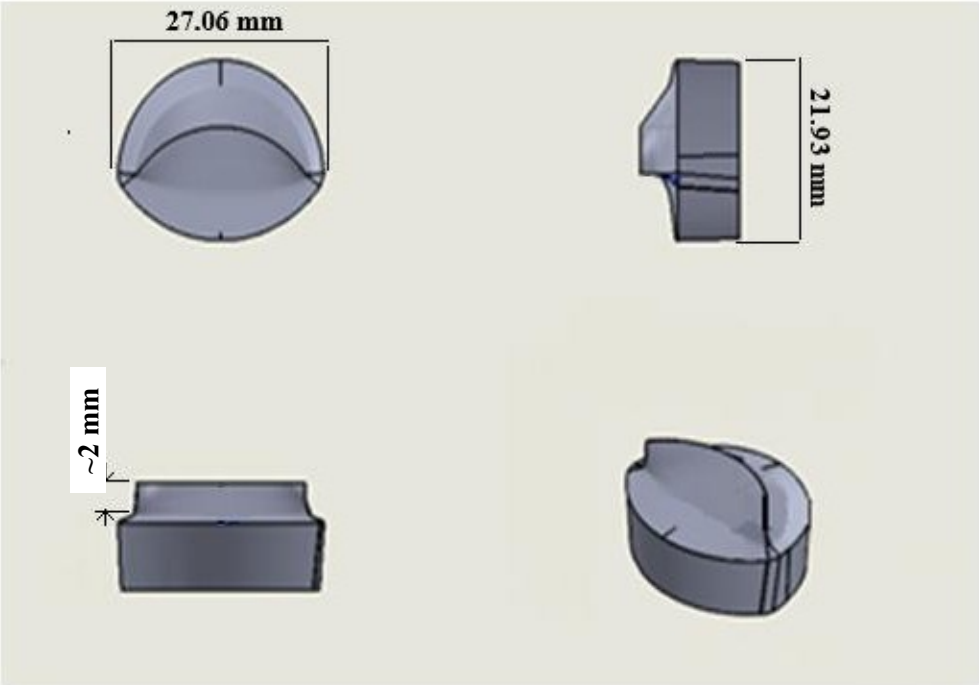

Figure 3-5. The CAD design of the mitral valve leaflets mold.

As can be seen in figure 3-5, in order to avoid mitral valve prolapse, the edges of the leaflets were designed to have an approximate 2 mm coaptation surface.

Figure 3-6. 3D printed mitral valve leaflets mold, printed by a FDM printer, Lulzbot Taz 6, with a PLA filament

The next step to fabricating the designed valve was to sew the leaflets and the stent together. In order to avoid future leaflet rips or any leakage, one layer of silicone was applied on the stitches.

3.2.3. Chordae Tendineae

Considering the thickness of the leaflets which was approximately 0.7 mm, the optimum number of the artificial chordae tendineae on each of the leaflets was decided to be three. This would guarantee the perfect leaflet coaptation without facing leaflet rips under fluid pressure during either diastole or systole. Therefore, six cords, three per leaflet, were created in order to connect the free edges of the leaflets to the stent wall, with an angle of 45º. Each of the cords consisted of two cotton strings braided together. At the end of the process, silicone drops were applied to tighten the ends of the cords situated on the leaflets and on the stent walls. Figure 3-7 illustrates the CAD designs of the mitral valve.

Figure 3-7. Mitral valve CAD drawing including the artificial chordae tendineae

Figure 3-8. Mitral valve before attaching the artificial chordae tendineae

Following the required rest time for the silicone drops to completely cure, the stent was sewn to the ventricle wall, in the position of mitral valve (Figures 3-9, 3-10). For the purpose of avoiding leakage through the ventricle, a thin layer of silicone was again applied on the stitches.

Figure 3-9. Placement of mitral valve in the left ventricle

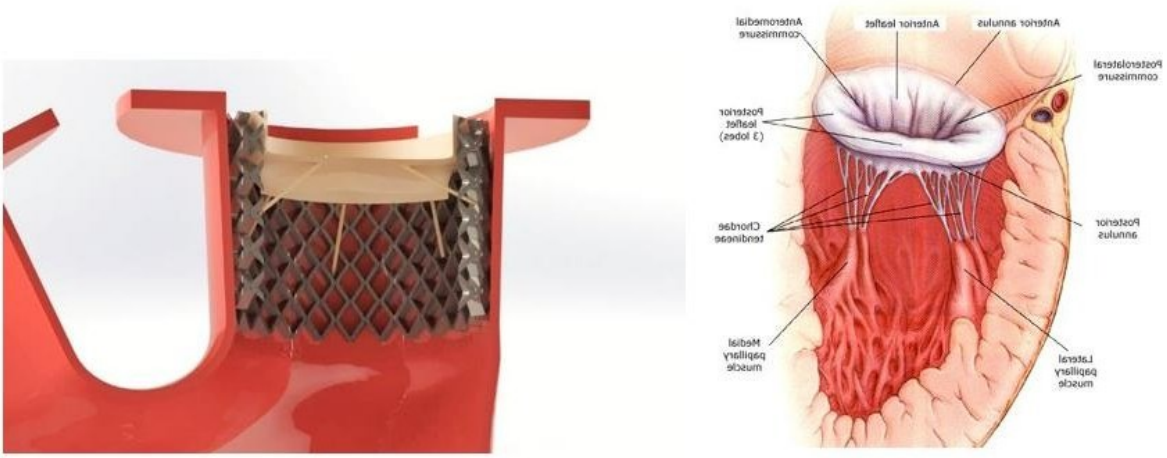

Figure 3-10. A comparison between placement of the native mitral valve [9] and the designed mitral valve in the left ventricle

3.3. *In Vitro* Setup

3.3.1. Blood Analogue

Blood viscosity is dependent on various parameters such as the volume percent of red blood cells, shear rate and even vessel diameter. But for shear rates above 100 s^{-1}, viscosity becomes constant and blood can be considered as a Newtonian fluid. This is the case in large arteries and cavities like the left ventricle. In this regard, the fluid used in the simulator, to mimic blood characteristics, was a mixture of water and glycerol with a mixture ratio of 6:4 by volume. This mixture has a dynamic viscosity of 4.2 cP and a density of 1080 kg/m^3, which is close to the reported values for blood properties in large arteries.

3.3.2. Cardiac Simulator

A custom-made heart duplicator was used in this experimental work. The simulator is capable of reproducing flow and pressure conditions that are similar to those obtained in humans under healthy and pathological conditions. It consists of an open tank (reservoir) located at a higher level and is connected to the left atrium through tubing and sets of valves. In this setup, the flow goes from the open tank to the left atrium, through the mitral valve, and then to the left ventricle. For the purpose of mimicking the left ventricle myocardium, a piston-cylinder assembly is employed. The movement of the piston reproduces the contraction and expansion of the left ventricle. The flow in the left ventricle is pumped towards the outflow tract through an aortic valve

(27A-101, St. Jude mechanical Regent^{TM}, 24.9 mm) and to the aorta. Finally, the fluid is returned to the reservoir. A servo motor (RX24F dynamixe, Robotis, USA) was employed to simulate the left atrium kick or A-wave. The simulator is controlled using a custom-made Labview program (National Instruments, Texas, USA). This allows for the reproduction of several heart conditions in terms of heart rate and stroke volumes. On the simulator, the cardiac output was measured by a magnetic inductive flowmeter (Automation Direct, Georgia, USA) placed on the tube connecting aorta and the reservoir The pressure in the aorta was measured using a fiber optic pressure sensor (FISO, Quebec, Canada).

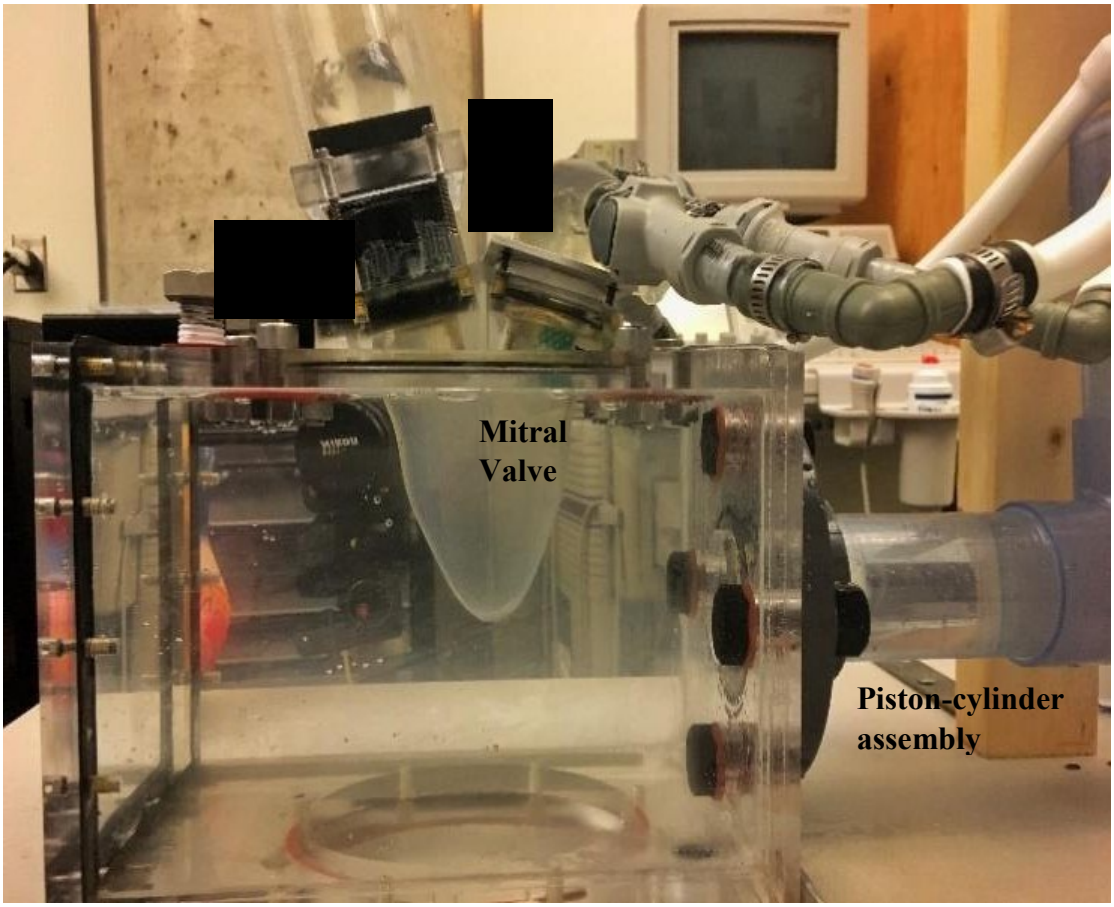

Figure 3-11. The cardiac simulator system. The piston-cylinder assembly is responsible for left ventricle contraction and expansion

3.4. Particle Image Velocimetry Measurements

The effects due to the presence of in-stent artificial chordae tendineae on flow characteristics in the left ventricle was evaluated by measuring the velocity field in the left ventricle using particle image velocimetry (PIV). PIV is an optical method for flow observation used to obtain instantaneous velocity measurements and related properties in fluids. It has already been applied in different research fields e.g. biomedical (cardiovascular fluid dynamics), environmental (wave dynamics, coastal engineering), hydrodynamics (velocity measurement in water flows) and aerodynamics (testing aircrafts). A standard PIV system requires a light source, digital high speed camera(s) and light scattering particles (see Figure 3-12).

For planar velocity measurements, two consecutive images are recorded by a single high speed camera, within a determined time delay (dt) while a laser illuminates the seeded fluid so that particles are visible. Since there are a high number of particles in each image, the frames are divided into interrogation areas (typically 32 by 32 pixels or less) and cross-correlation is performed between the two frames. The peak of the cross-correlation in each interrogation area gives the displacement of the particles within the specific area. Using this information and the determined time delay, the velocity field of the flow can be determined.

In this study, PIV has been used to investigate the velocity field inside the left ventricle in the presence of the new designed mitral valve.

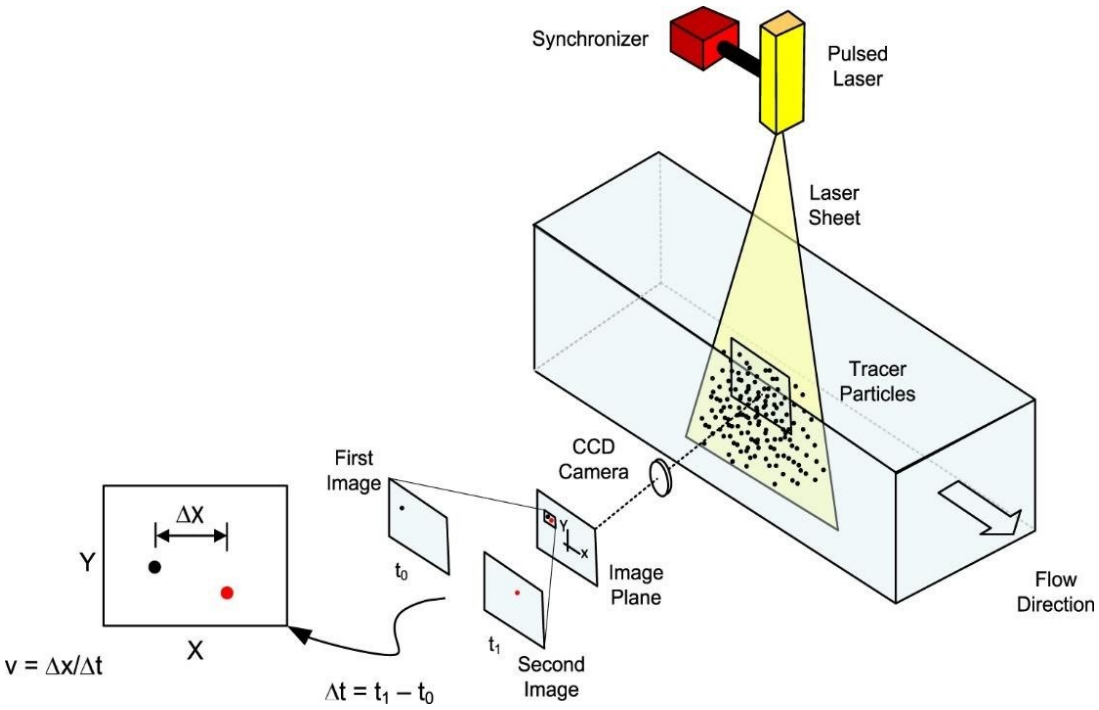

Figure 3-12. Schematic diagram of the PIV technique [68]

A LaVision PIV system (LaVision GmbH, Goettingen, Germany) was used in this study with a dual cavity Nd: YLF laser (Litron Lasers, Warwickshire, UK) with a maximum repetition rate of 20 kHz and a maximum pulse energy of 10 mJ at 527 nm. The laser sheet, with a thickness of 1 mm; was positioned parallel to the mid-plane of the left ventricle, so that the particles could be traced entering and leaving the ventricle through the mitral and the aortic valves, respectively.

In PIV, the selection of the seeding particles is a very important step. In addition to considerations such as choosing non-toxic, non-corrosive, and chemically inert seeding particles, there are some other conditions that should be mentioned. The seeding particles should be small enough to be good flow tracers (reduction of Stokes drag), yet large enough to scatter sufficient light for imaging. The PIV method is optimal with a medium seeding particle density compared to other optical based methods like laser speckle velocimetry or particle tracking velocimetry methods [69]. Another important property required from the seeding particles, particularly for cardiovascular flow applications, is their time response. They have to be capable of rapidly responding to sudden variations in flow velocity [70]. In this study, polyamide seeding particles

of 20 µm diameters and a density of 1.03 g/cm³ were found to adequately adhere to the above mentioned conditions.

A Phantom v9.1 camera (Vision Research, Stuart, FL, USA) with 1000 frames per second at a maximal resolution of 1632×1200 pixels was used for recording the images. In order to optimize the cross-correlation of the PIV measurements for each instant of measurement, the time step between two consecutive laser pulses was decided to be in the range of 400-500 µs. A total of 343 pairs of images were recorded for each series of experiments. A cross-correlation was used with an initial interrogation area of 64×64 pixels, and a final size of 32×32 pixels, with 50% overlapping. Table 3-3 summarizes the selected parameters for the PIV measurements.

A depiction of the placement of PIV setting devices used for the experiments is shown in figure 3-13.

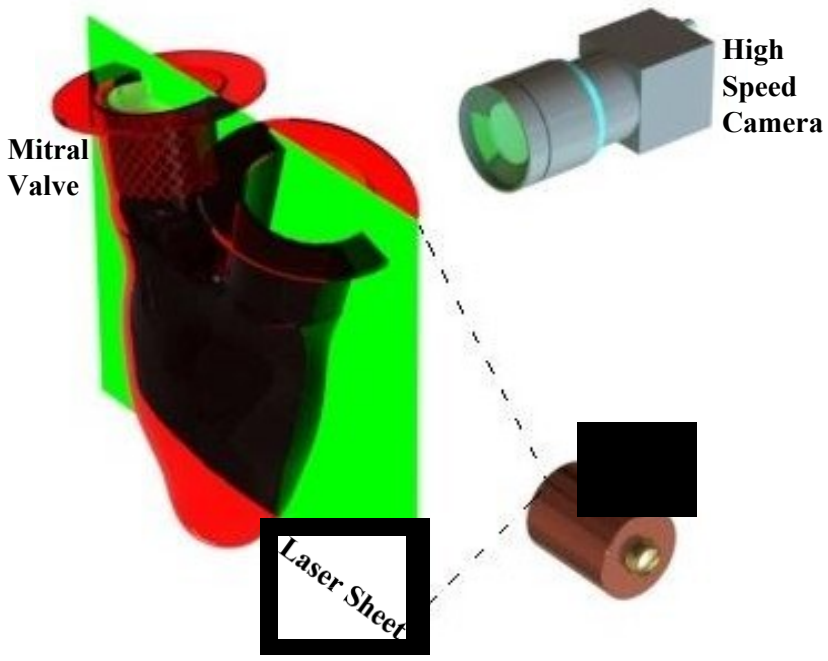

Figure 3-13. Position of the PIV devices for velocity measurements. The camera lens is prependicular to the laser sheet

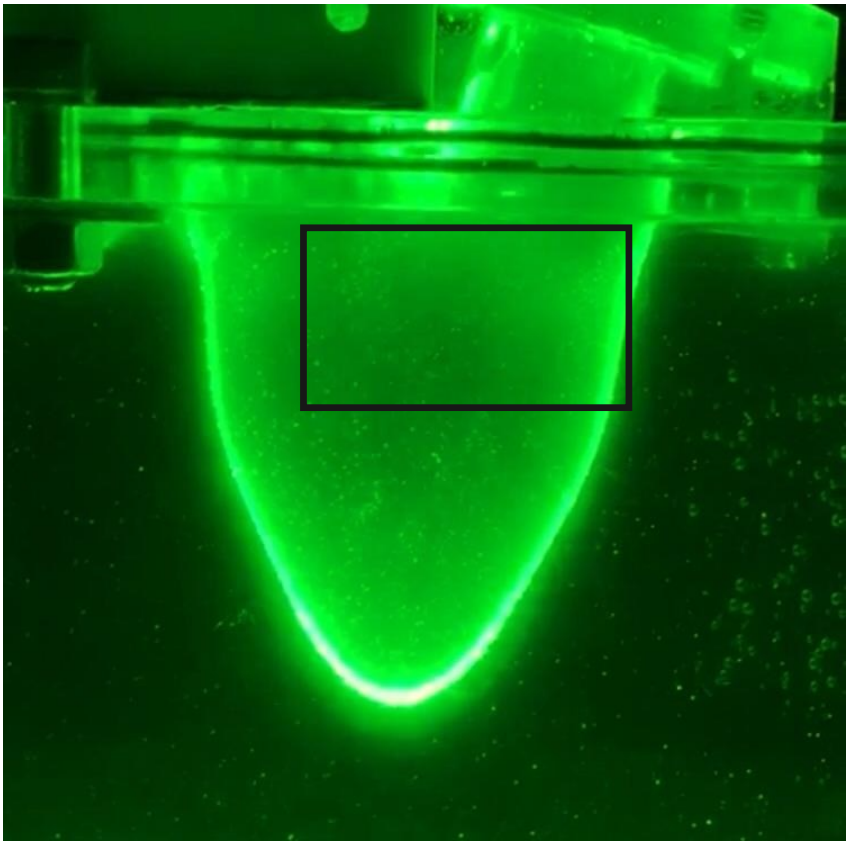

Figure 3-14. Picture of the left ventricle as illuminated by the laser sheet. The black box shows the region of interest were velocity measurements are performed.

Table 3-3. PIV measurements parameters

Condition	Value
Cardiac cycle duration	0.857 s
dt between laser pulses	400-500 μs
Frequency of images	400 s^{-1}
Number of images per cycle	2×343

3.4.1. PIV Uncertainty Analysis

Raffel et al. quote many parameters that can affect the accuracy of PIV, such as particle image density, particle image diameter, particle displacement, and shear [71]. In case of considering a particle displacement only in the X and Y directions, the major uncertainty in the velocity measurement could be presented by the uncertainty in geometric parameters and image displacement. However, flow fields cannot be practically considered two-dimensional over the whole observation field [72].

Tables 3-4 and 3-5 present other contributing factors in PIV uncertainty [73].

Table 3-4. Evaluation of the uncertainty of the PIV velocity [73]

Parameter	Error sources	U_i=Standard Uncertainty	C_i=Sensitivity Coef	U_i*C_i
α	Magnification factor	0.002169007	1667	3.6
Δx	Image displacement	0.382197398	23	8.9
Dt	Image interval	5.38516E-09	38889	0.0
du	Experiment	5.38516E-09	1	5.38516E-09

Table 3-5. Contributing factors in PIV uncertainty [73]

Parameter	Category	Error Source	U_i=Standard Uncertainty	C_i=Sensitivity Coef	U_i*C_i	Combined Uncertainty
α (mm/pix)	Calibration	reference image	0.7	3.75E-04	2.63E-04	0.0036581
		physical distance	0.02	1.25E-03	2.50E-05	
		Image distortion by lens	4	3.75E-04	1.50E-03	
		Image distortion by CCD	0.0056	3.75E-04	2.10E-06	
		board position	0.5	3.00E-03	1.50E-03	
		Parallel board	0.035	1.05E-02	3.68E-04	
Dx (pix)	Acquisition	Laser power fluctuation	0.0071	1.79E+01	1.27E-01	0.382197398
		Image distortion by CCD	0.0056	5.60E-02	3.14E-04	
		Normal view angle	0.035	1.05E-02	3.68E-04	
	Reduction	Mismatching error	0.2	1.00E+00	2.00E-01	
		Subpixel analysis	0.3	1.00E+00	3.00E-01	
Δt (s)	Acquisition	Delay generation	2.00E-09	1	2.00E-09	5.38516E-09
		Pulse time	5.00E-09	1.00E+00	5.00E-09	
δu (mm/s)	Experiment	Particle trajectory	0.015	1	0.015	0.81959101
		3-D effects	0.819453735	1	0.819453735	

According to the tables above, the uncertainty on PIV measurements is 0.00962 m/s, which is translated into 6.4%.

3.5. Experimental Conditions

In order to evaluate the performance of the newly designed mitral valve, two series of experiments were performed. The objective of the experiments was to determine the impact of the presence of the in-stent artificial chordae tendineae on the flow in the left ventricle model. In order to limit confounding factors, the same valve design was used and measurements were performed first with the in-stent chordae tendineae and then were performed once again after the chordae tendineae were removed. Of interest were leaflet coaptation, mitral valve regurgitation and flow structures in the left ventricle.

Each set of experiments was repeated for at least 5 times to make sure of the repeatability of the results. In all experiments, the heart rate was kept at 70 beats/min and the cardiac output at 4.3 L/min with the corresponding piston stroke of 40 mm and the trigger starting with the left ventricular systole. The systolic/diastolic aortic pressures were maintained in a physiological range (120/80 mmHg) in the presence of the artificial chordae tendineae.

Chapter 4

Results

The purpose of this chapter is to present the results of the *in vitro* experiments performed on the newly designed mitral valve, both in the presence and the absence of the artificial chordae tendineae. A comparison between the two cases, in terms of velocity fields and particle trajectories, velocity profiles and mitral regurgitation will be performed.

4.1. Aortic Pressure

The experimental setup described in chapter 3 was adjusted to provide ideal physiological conditions for the aortic pressure and a cardiac output at a heart rate of 70 bpm under normal conditions. The aortic pressure for the first set of experiments with the artificial chordae tendineae is illustrated in Figure 4-1.

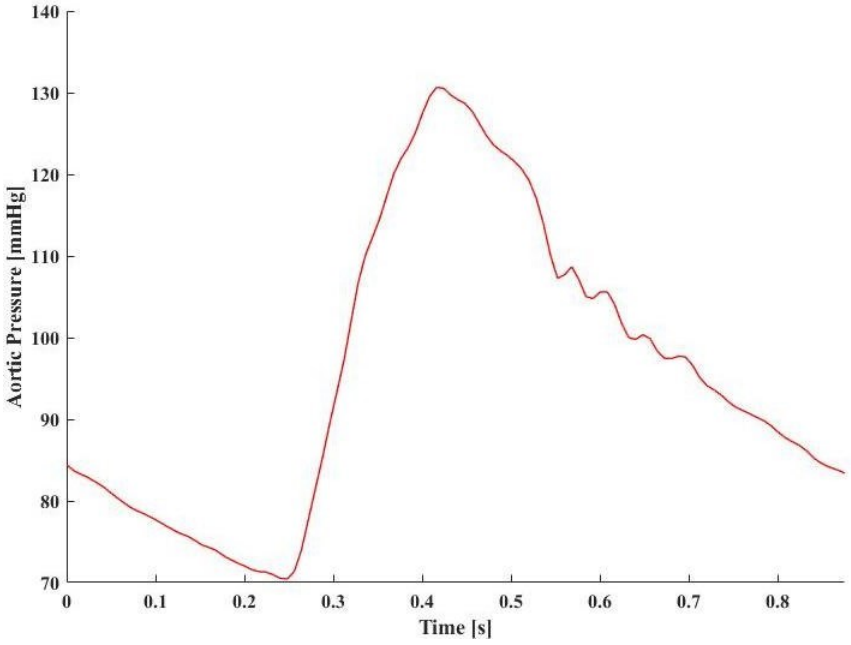

Figure 4-1. Aortic pressure for one cycle, measured during the experiment

4.2. *In vitro* experiments

Figure 4-2 shows leaflet coaptations of the mitral valve in the presence and absence of the artificial chordae tendineae, during left ventricular contraction. The pictures represent snapshots extracted from the videos recorded during the sets of experiments, both with and without the artificial chordae tendineae. The comparison between the two snapshots shows that the addition of the artificial chordae tendineae leads to a better performance of the mitral valve in terms of leaflet coaptation. However, more detailed analyses are required in order to better evaluate the independent effect of the chordae tendineae on mitral valve performance, particularly in prevention of mitral regurgitation. More specifically, measurements were performed in order to evaluate the flow characteristics in detail and quantify the amount of mitral regurgitation.

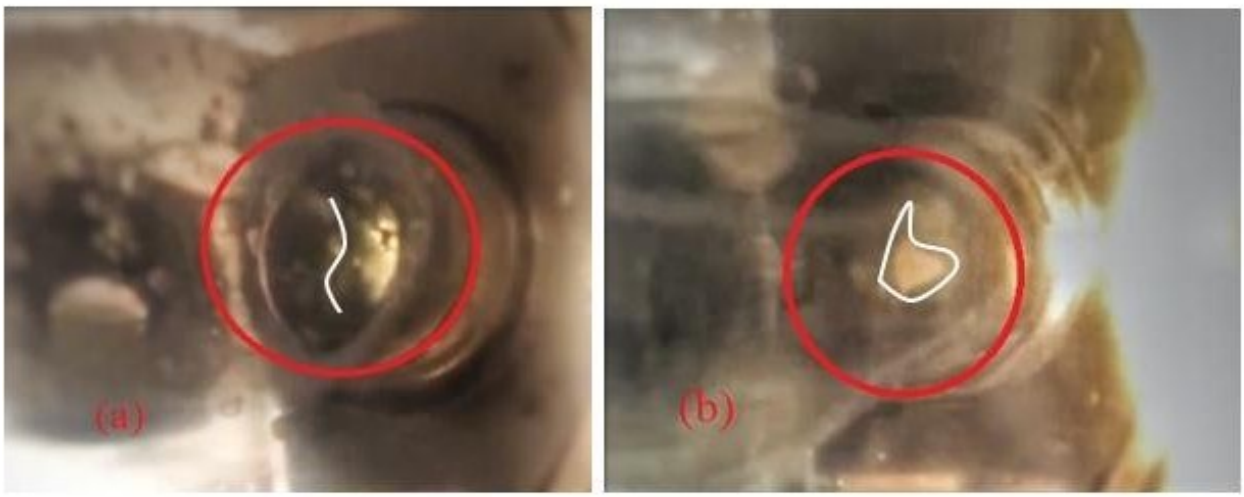

Figure 4-2. Comparison between the leaflets coaptation, during systole a) in presence of the chordae tendineae, b) in absence of the chordae tendineae. The white lines are simple illustrations of the coaptation of the leaflets

4.2.1. Velocity fields

Velocity fields inside the left ventricle during systole were obtained using time-resolved particle image velocimetry. In order to limit the post-processing to the region of interest, i.e. inside the left ventricle, a mask was applied. The field of view comprises the whole entrance area of the mitral valve and the right half of the aortic valve entrance area which is adjacent to the mitral

valve. The purpose of recording the velocity field was to observe the flow patterns in the left ventricle with and without the artificial chordae tendineae. Since mitral regurgitation is the focus of this study, instants from early and late systole were selected, so that the flow pattern before ejection from the ventricle could be observed.

According to Figure 4-3, a physiologically realistic flow swirling, in the form of one unique vortex in the left ventricle is present at the onset of left ventricle ejection. The flow already entered the ventricle through the mitral valve, participates in a clockwise vortex formation before it leaves the ventricle through the aortic valve. The contribution of the artificial chordae tendineae becomes more outstanding when the pressure in the left ventricle increases. At this moment, the flow leaves the ventricle towards the ascending aorta. The flow pushes the mitral valve leaflets towards the left atrium, while the chordae tendineae pull the leaflets towards the left ventricle. This leads to a complete coaptation of the valve leaflets as well as prevention of mitral prolapse and consequently, mitral regurgitation. This leaves the aortic valve as the only possible exit for the flow. Therefore, there is a smooth redirection of the flow from the mitral valve towards the aortic valve.

In absence of the chordae tendineae, as it is illustrated in Figure 4-4, the flow tends to leave the ventricle through both the aortic and mitral valves, this is the result of mitral valve prolapse leading to significant mitral valve regurgitation. In addition, during mid and late systole, a large number of small-scale vortices start to appear and no specific flow patterns can be detected. It can be concluded that the absence of the chordae tendineae not only leads to mitral prolapse during systole, but also can cause disturbed flow in the LV which results in high energy losses. The lost kinetic energy needs to be provided by the ventricular musculature [59] (Figure 4-5).

4.2.2. Vortex Extraction

Vortex extraction presents one of the most important and challenging aspects of fluid flow observations. Among all the subjects discussed in vortex definitions, two of them are mentioned most often and are still actively researched. All of these definitions require the definition of a vortex coreline, i.e. a line around which particles rotate, and an appropriate selection of a reference frame, in which the velocity field becomes steady.

For a 2D flow, Graftieaux et al. presented the Γ_2-criterion. At each point x, they defined a rectangular area S around it [74]. They sampled area S with points y and define Γ_2 as

$$\Gamma_2(\mathrm{x}) = \frac{1}{|S|} \int_{y \in S} \sqrt{1 - \left(\frac{(v(y) - v_{avg}(y))^T (y - x)}{\|v(y) - v_{avg}(y)\| \cdot \|y - x\|} \right)^2} \, dS$$

By that definition, $v_{avg}(y)$ is the average velocity in a stencil around y, which is used to relate the velocity to the neighborhood using that Galilean invariant. The selection of the size of both region S and the stencil radius for v_{avg} are of importance. This method determines whether the flow goes around point x by averaging the sine (with $\sin x = \sqrt{1 - \cos x^2}$) of the angle between the flow direction at y and the direction toward the sampled point x inside region S. If x happens to be on the coreline of an axis-symmetric vortex (e.g. a perfect centre), Γ_2 increases towards 1 [75].

In this thesis, the vortices formed in the left ventricle during systole, in both the presence and absence of the artificial chordae tendineae were detected, using the Γ_2-criterion (Figure 4-3, 4-4).

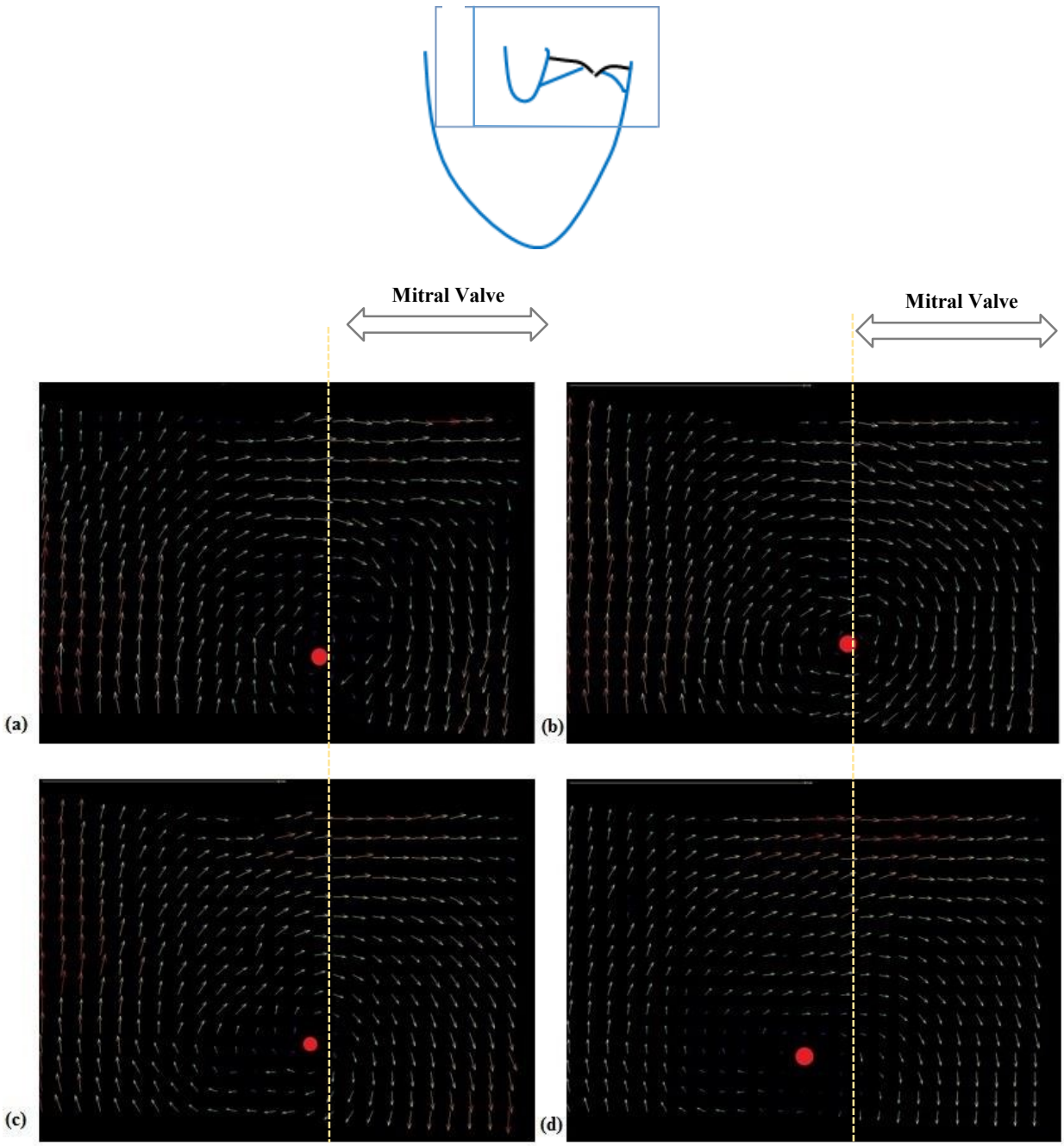

Figure 4-3. Velocity fields in the left ventricle and formation of one unique vortex, in presence of the artificial chordae tendineae during (a) early systole; (b) mid systole; (c), (d) late systole. Due to the good coaptation of the mitral valve leafets, the flow in the left ventricle moves in a natural pattern, inducing no backflow into the left atrium

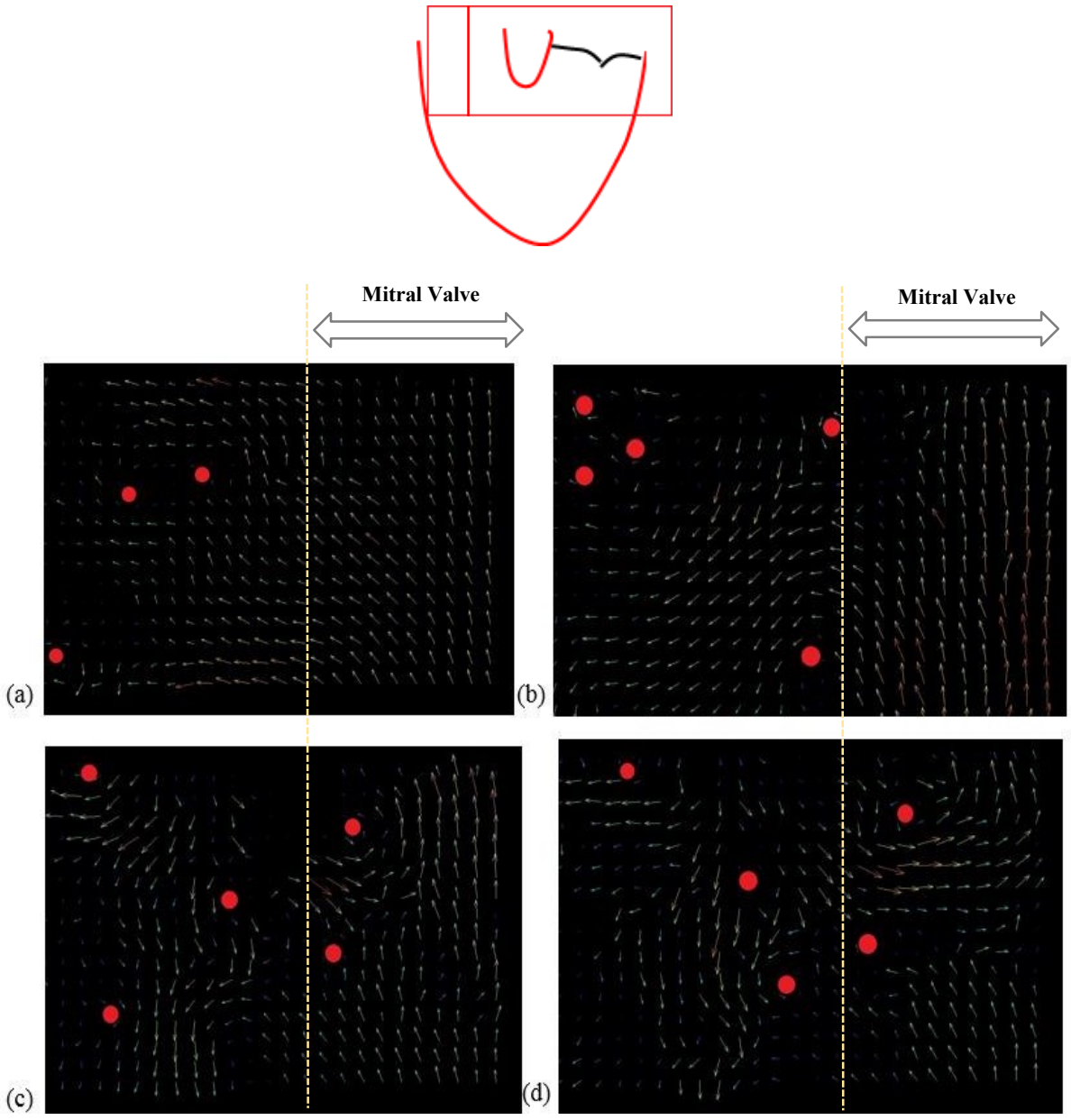

Figure 4-4. Velocity fields in the left ventricle in the absence of the artificial chordae tendineae during (a) early systole; (b) mid systole; (c), (d) late systole. The tendency of the flow for leaving the left ventricle through mitral valve can be seen in this figure. This is due to the significant mitral valve prolapse in the absence of the artificial chordae tendineae. It can be observed that numerous small-scale vortices are formed and no certain flow pattern can be detected. Interaction of the vortices leads to large amounts of viscous energy dissipation

Due to fluid viscosity, interaction of vortices in the left ventricle can lose energy. Rapid changes in vorticity (high pulsatility) or presence of many small vortices (turbulence) can lead to high energy losses, while presence of one single large and steady vortex can result in an energetically desirable condition. In other words, separation of the bloodstream into smaller rapidly altering vortices is not favorable [59]. Figure 4-5 illustrates the viscous energy dissipation in the presence and absence of the artificial chordae tendineae. As expected, the amount of viscous energy dissipation in the absence of the artificial chordae tendineae is larger compared to the case in which the artificial chordae tendineae are present. The average amount of viscous energy dissipation in the two cases and the standard deviation is shown in figure 4-6. According to the computed p-value, it can be concluded that the two cases are statistically different.

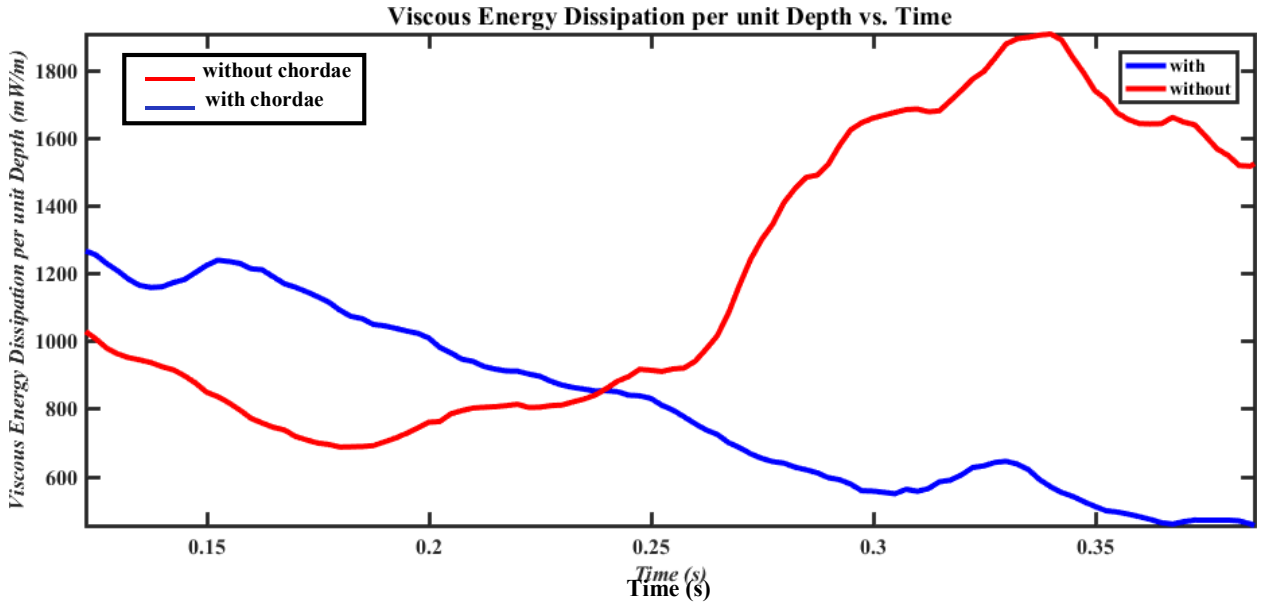

Figure 4-5. Comparison between viscous energy dissipation per unit depth in presence and absence of the artificial chordae tendineae, during systole

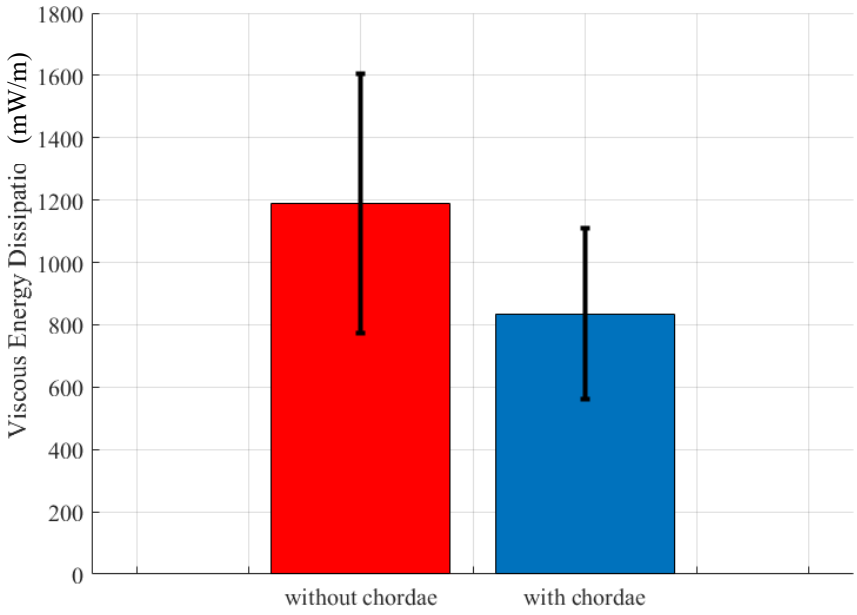

Figure 4-6. Average value of energy viscous dissipation during systole and the standard deviation ($p < 0.001$)

Figures 4-7 to 4-10, illustrate the magnitude of the vertical and horizontal components of the velocity vectors in the velocity fields, indicated as Vy and Vx respectively. The data are recorded in the presence and absence of the chordae tendineae at several instants during early systole, mid systole as well as late systole so that the flow pattern can be observed thoroughly. By taking a closer look at the entrance area of the mitral valve, the magnitude of the Vy components in the presence of the chordae tendineae is very close to zero. This means that the angle between each velocity vector and the horizontal axis in that particular area is either zero or negative. Therefore, the flow is not expected to move towards the mitral valve during systole. At the same time, it can be seen that the maximum Vy in presence of the chordae tendineae happens in the left ventricle outflow tract just upstream from the aortic valve entrance area which is in agreement with the presence of a natural flow during systole and the absence of mitral regurgitation. In addition, relatively large magnitudes of Vx adjacent to the mitral valve, in presence of the artificial chordae tendineae, is in agreement with the natural flow direction in a healthy human heart.

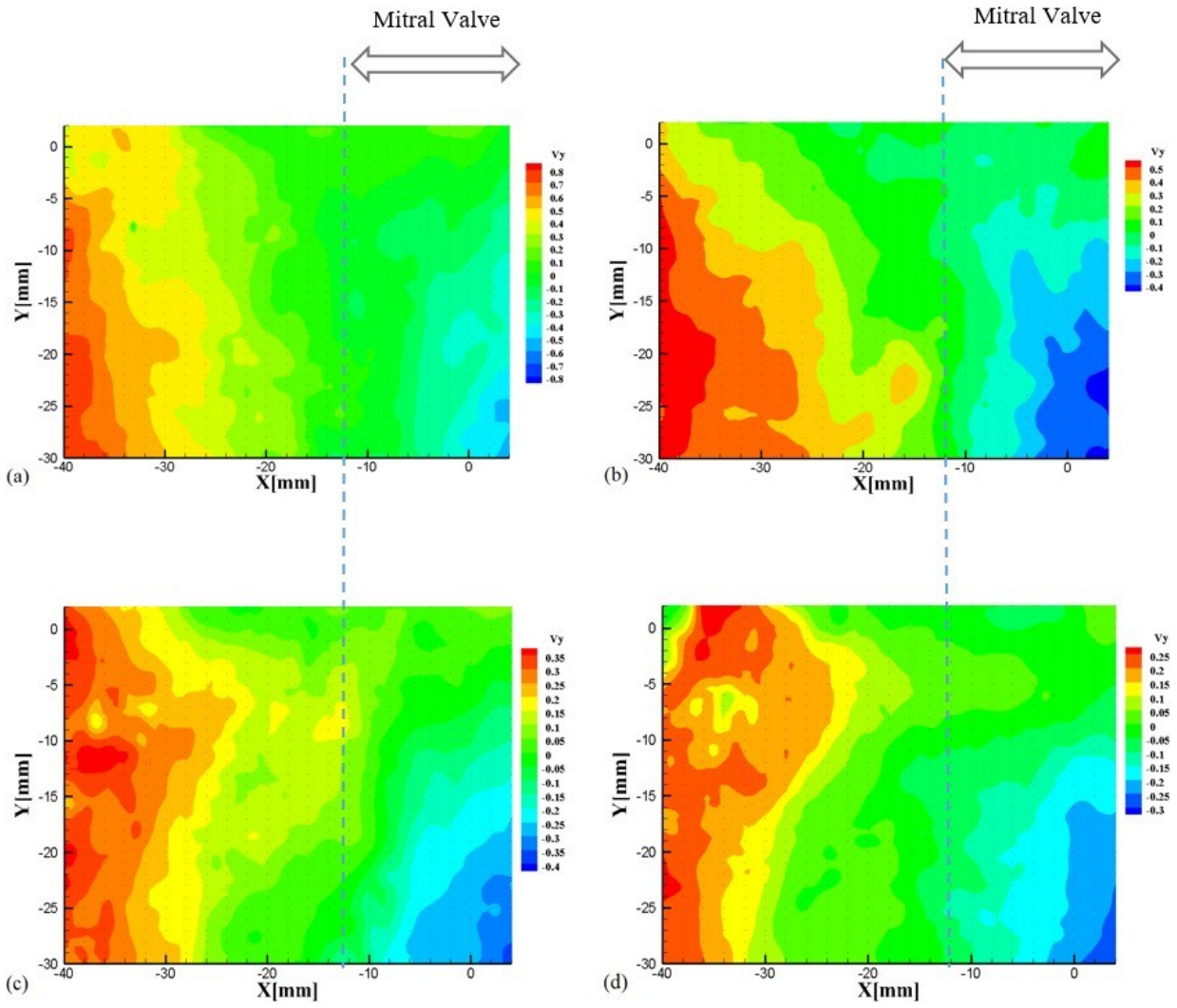

Figure 4-7. Vy (m/s) contours for several instants, in the left ventricle with a mitral valve with artificial chordae tendineae, during a) early systole, b, c) mid-systole, d) late systole. It can be seen that Vy component of the velocity vectors are large in the aortic side of the LV and small in the mitral side, which indicates the tendency of the flow for leaving the LV only through the aortic valve

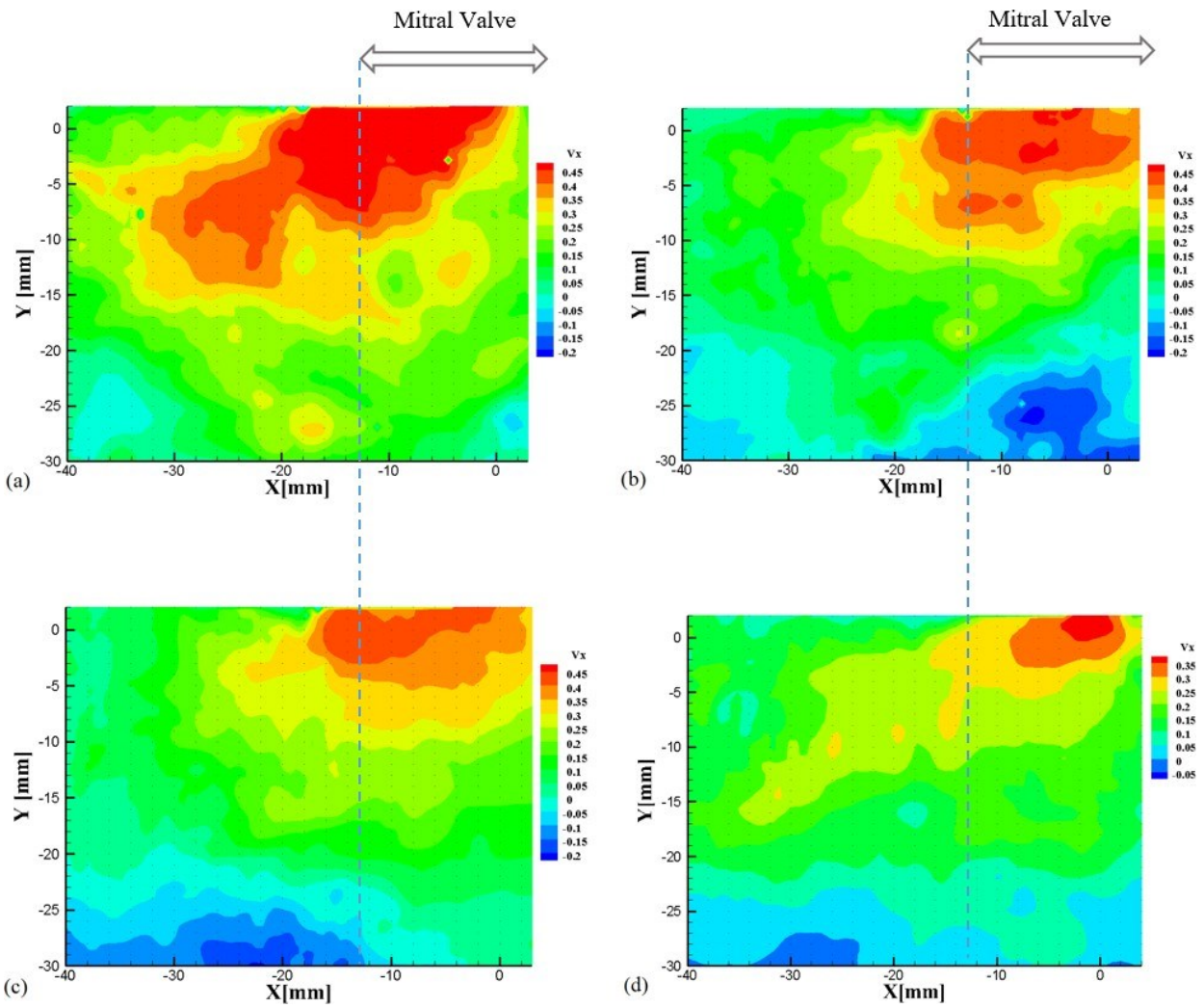

Figure 4-8. Vx (m/s) contours for several instants, in the left ventricle with a mitral valve with artificial chordae tendineae, during a) early systole, b, c) mid-systole, d) late systole. As it is indicated in this figure, the magniude of the Vx components are large in the regions close to the mitral valve. This is in agreament with the physiological flow direction in the LV, expected in the presence of the artificial chordae tendineae

In contrast, in the case when there are no chordae tendineae, Vy components adjacent to the mitral valve have a large positive upward magnitude (Figure 4-9). On the aortic side, Vy components have mostly negative downward values indicating that the flow tends to move away from the aortic valve. This shows that a large amount of the flow exits through the mitral valve and a relatively small amount of the flow exits through the aortic valve during systole, which is not physiologically realistic.

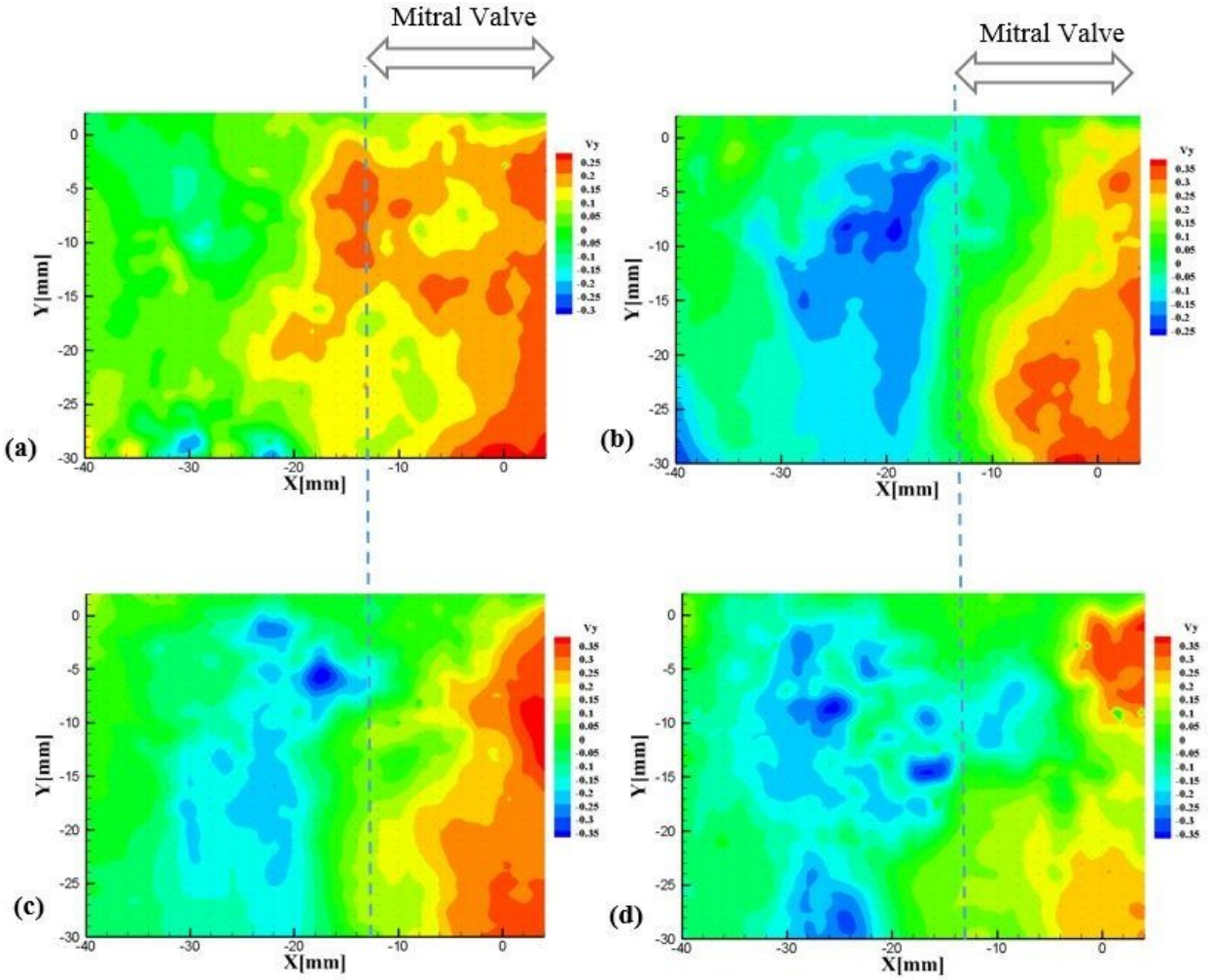

Figure 4-9. Vy (m/s) contours for several instants, in the left ventricle with a mitral valve without artificial chordae tendineae, during a) early systole, b, c) mid-systole, d) late systole. According to this figure, Vy components adjacent to the mitral valve own a large positive upward magnitude while having a small magnitude in the regions close to the aortic valve. This indicates the tendency of the particles for leaving the LV through mitral valve

In the absence of the artificial chordae tendineae, as it is illustrated in Figure 4-10, different values of the Vx component is detected at different instants in the same regions. According to this figure, no particular flow pattern can be found in the absence of the artificial chordae tendineae, and the flow in the LV is chaotic.

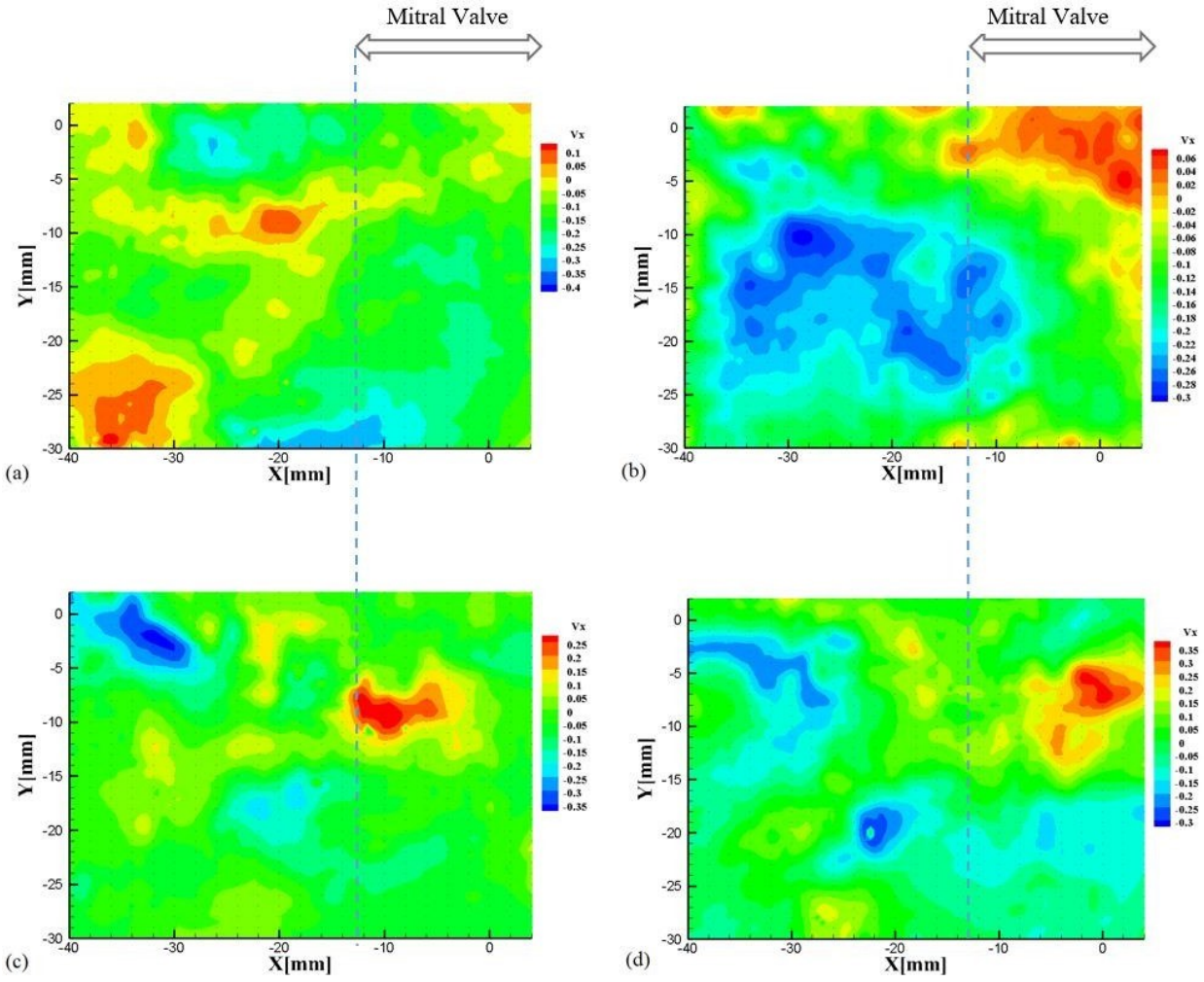

Figure 4-10. Vx (m/s) contours for specific instants, in the left ventricle with a mitral valve without artificial chordae tendineae, during a) early systole, b, c) mid-systole, d) late systole

4.2.3. Velocity profiles

In Figures 4-11 and 4-12, Vy profiles at selected instants of systole are plotted in the presence and absence of the artificial chordae tendineae. Considering Figure 4-11, the vertical components of the velocity vectors in the aortic side are positive, with relatively large values while their values close to the mitral valve area are small and mostly negative i.e. pointing downwards. This represents the tendency of the flow to move in a horizontal or downward direction when close to the mitral valve and in an upward direction when close to the aortic side. It can be concluded that almost all the flow leaves the ventricle through the aortic valve in the presence of the artificial chordae tendineae, hence no mitral regurgitation is noticeable.

By removing the artificial chordae tendineae from the mitral valve, mitral prolapse occurs. Therefore, a low pressure path towards the left atrium is available to the flow. This can be noticed on Figure 4-12, since the vertical components of the velocity vectors have positive values, and hence have upward directions in both mitral and aortic valves regions. It is also worth noticing that at some instants, the flow has a larger velocity magnitude in the mitral valve region than in the aortic valve region. This is the result of having the left atrium at a lower pressure than the aorta.

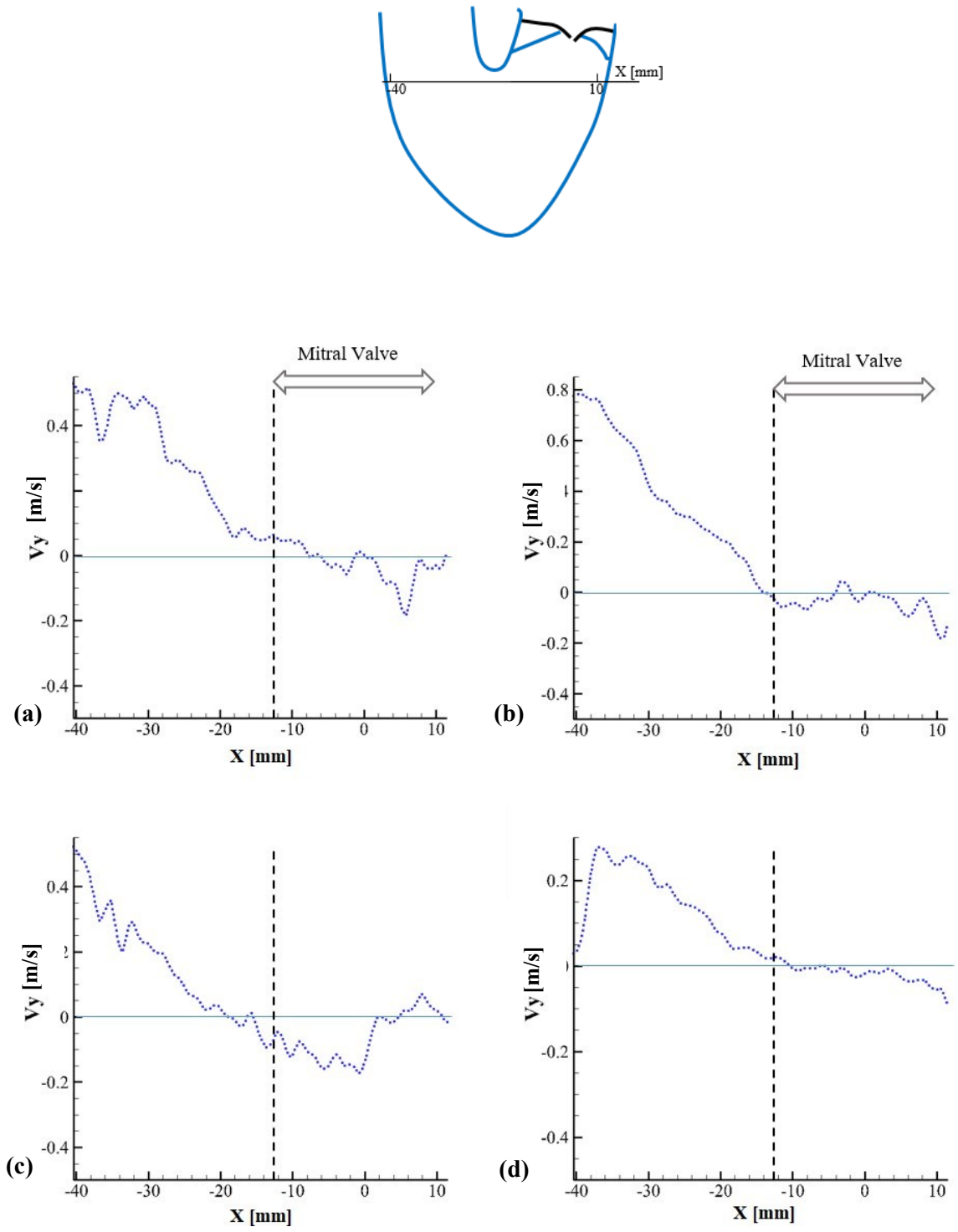

Figure 4-11. Vy profiles of velocity vectors in presence of the artificail chordae tendineae, during a, b) early systole, c) mid-systole d) late systole

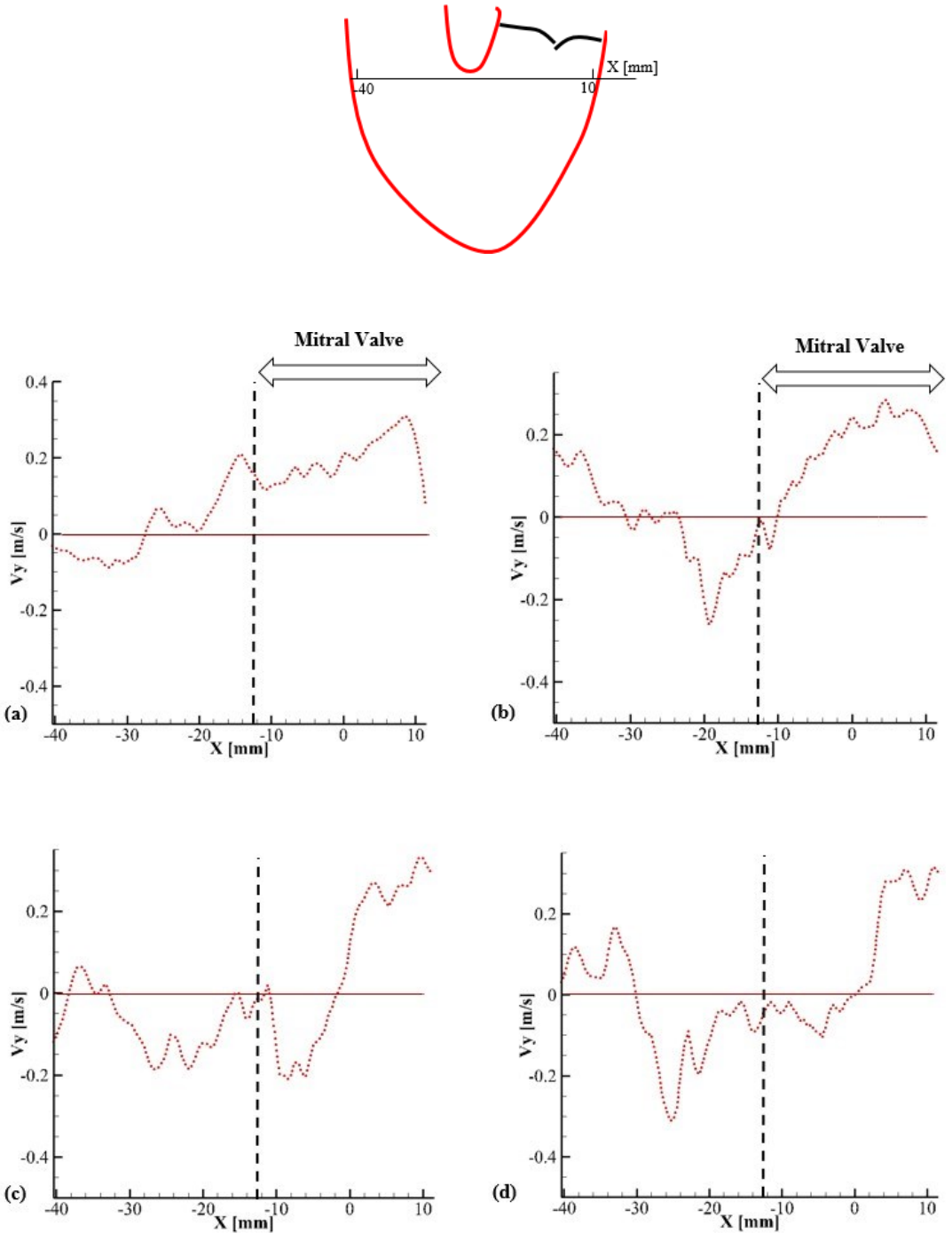

Figure 4-12. Vy profiles of velocity vectors in absence of the artificail chordae tendineae, during a) early systole, b, c) mid-systole d) late systole

4.2.4. Particle Trajectory

In order to take a closer look at the particles movements and the flow patterns in the left ventricle, tracers were advected at specific locations and followed during systole. For this purpose, the instantaneous velocity fields recorded before and after removing the artificial chordae tendineae, were used for particle advection.

Ten tracers starting from different locations in the field of view were considered to illustrate particle trajectories. Figures 4-13 and 4-14 demonstrate the particle paths in both cases during systole.

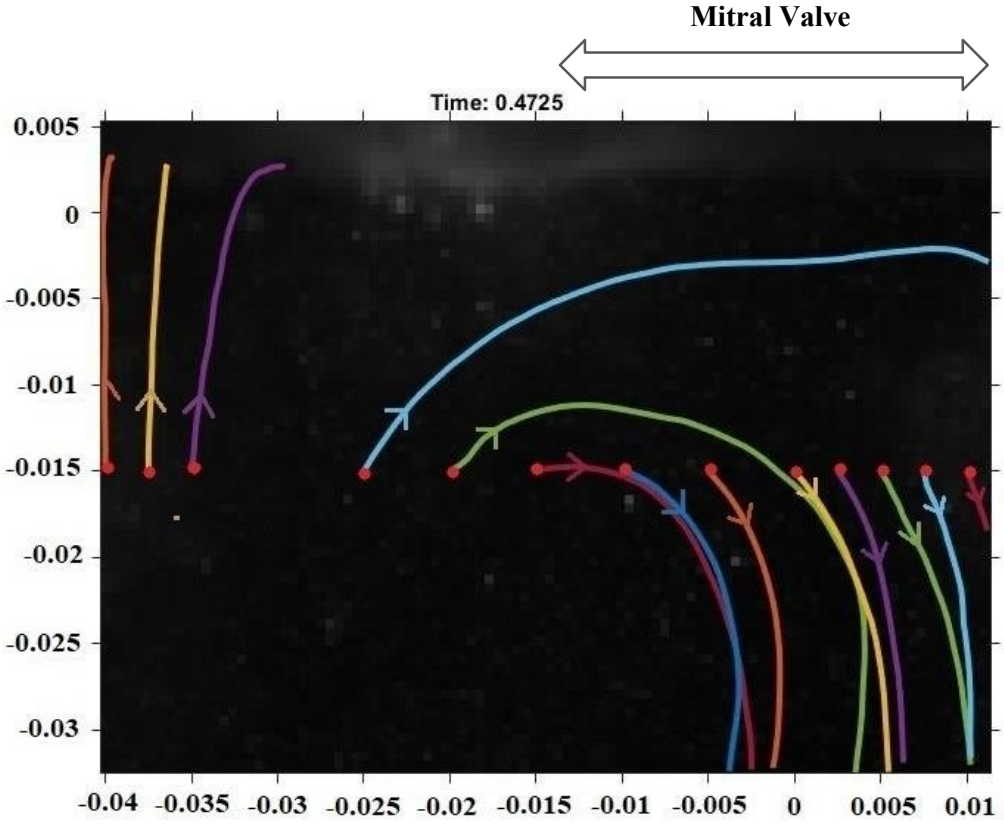

Figure 4-13. Particle trajectory during systole in the presence of the artificial chordae tendineae

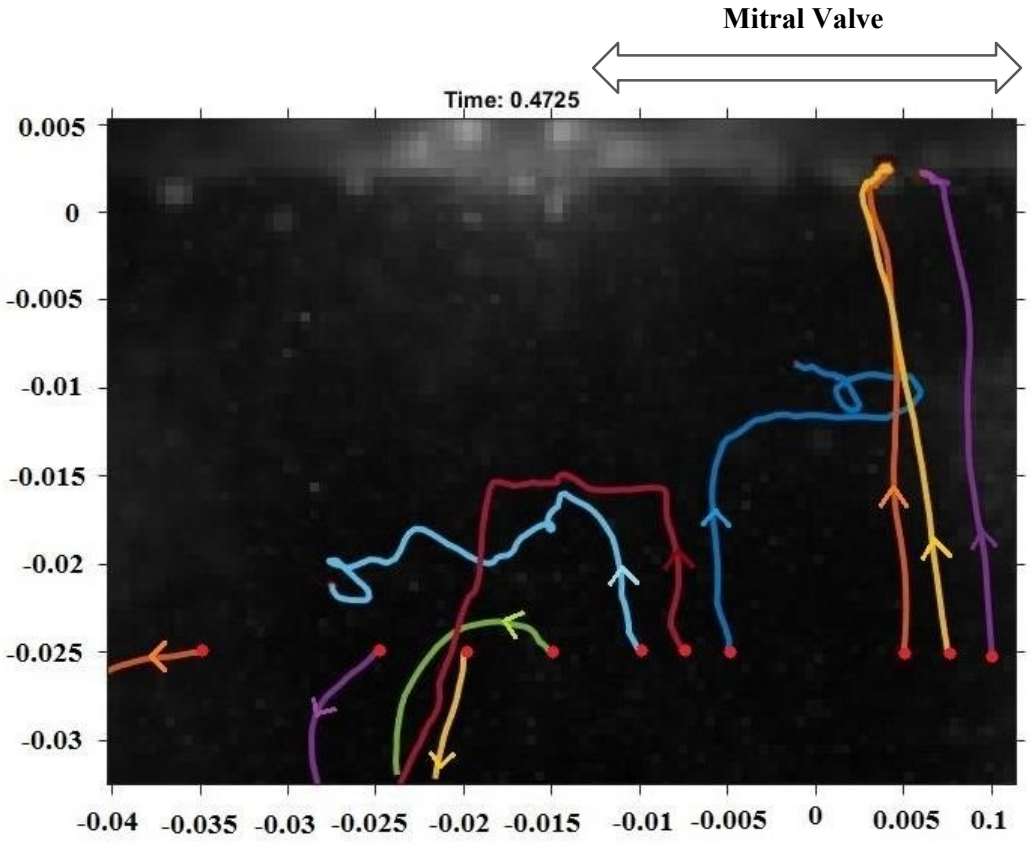

Figure 4-14. Particle trajectory during systole in the absence of the artificial chordae tendineae

As a result of complete coaptation of the leaflets, meaning the absence of mitral prolapse, the particles can only leave the ventricle during systole and through the aortic valve (Figure 4-13). In contrast, as can be seen in Figure 4-14, the absence of the artificial chordae tendineae creates another exit for the flow, through the mitral valve.

Other than the noticeable amount of mitral regurgitation, the phenomenon that is worth mentioning when comparing the two figures, are the flow patterns in the left ventricle. Although in both cases the same design was used and the only difference between them was the presence of the artificial chordae tendineae, there is a significant difference in the induced flow patterns in the left ventricle. According to figure 4-13, in the presence of the artificial chordae tendineae, flow moves in the form of one unique vortex, reproducing the physiologically natural flow pattern in a healthy human heart, while in the absence of the artificial chordae tendineae, the flow is “chaotic” and no specifically-defined flow pattern is observed.

4.2.5. Mitral regurgitation

In order to take a closer look at the velocity vectors close to the mitral valve, in the presence and absence of the artificial chordae tendineae, a particular area of the field of view that is very close to the valve was isolated. Vy components were averaged within this selected area and displayed as a function of time (Figure 4-15).

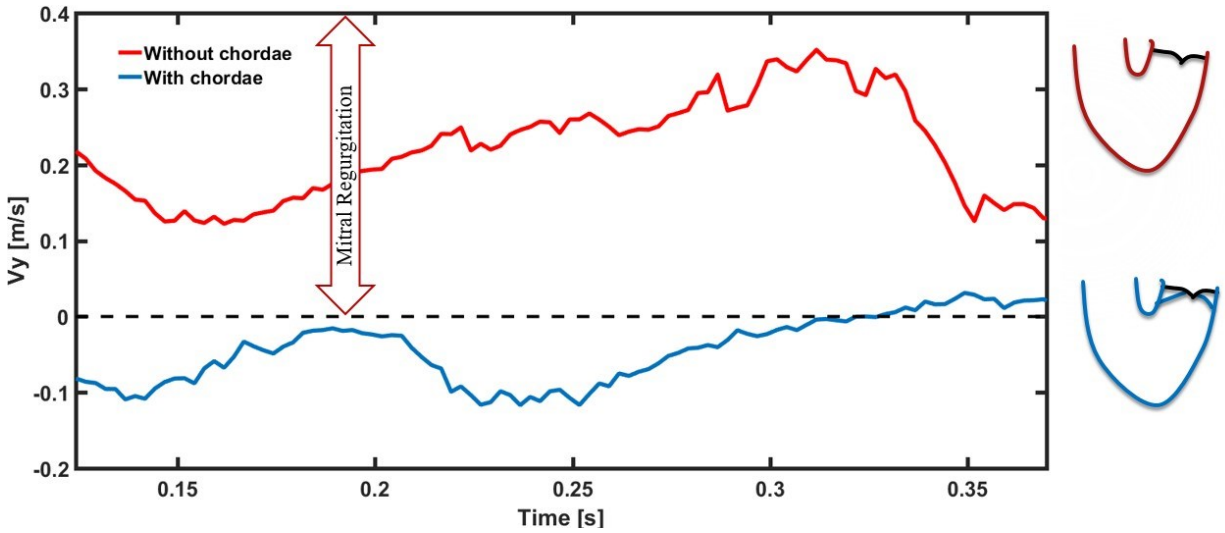

Figure 4-15. Comparison between the performances of the same mitral valve in different situations, in terms of mitral regurgitation

The magnitude of the upward velocity adjacent to the mitral valve entrance area is higher than zero during the whole systole while in the absence of the artificial chordae tendineae. This means that the flow tends to leave the ventricle through the mitral valve resulting in mitral regurgitation. In presence of the artificial chordae tendineae, however, the upward components of the velocity vectors have a negative value during almost the entire systolic phase. The very short period of time (> 0.32s), in which the Vy components are not negative, presents the time in which the flow moves in an almost horizontal direction. According to Figure 4-15, no mitral regurgitation can be detected in presence of the artificial chordae tendineae.

Chapter 5

Conclusion and Future Work

5.1. Summary and Conclusion

In this work, a novel transcatheter bileaflet mitral valve with in-stent artificial chordae tendineae was designed and tested. A cardiac simulator was used to study the performance of the designed valve as well as the cruciality of the presence of chordae tendineae as a part of the mitral valve apparatus under physiological conditions. PIV measurements were performed to obtain velocity fields. Velocity fields were then used to study viscous energy dissipation and mitral valve regurgitation. Particle tracking was also performed in order to trace the particles in the left ventricle while expansion and contraction during systole.

According to the acquired data, the number of formed vortices is higher in the LV in the absence of the artificial chordae tendineae. Interactions between the vortices, in the absence of the chordae tendineae, leads to a higher viscous energy dissipation compared to the situation in which the artificial chordae tendineae are present. Tracing the particles during systole, it became evident that in the absence of the chordae tendineae, particles tend to escape the ventricle through the mitral valve, while in the presence of the chordae tendineae, particles flow in a physiologically natural direction and leave the ventricle through the aortic valve. It can be concluded that artificial chordae tendineae play a crucial role in the performance of the designed mitral valve and that the next generation of transcatheter mitral valves should include in-stent chordae tendineae.

5.2. Future Work

There is still a long way to go regarding the research that was done in this thesis. Performing 3D flow measurements and optimization of the number and location of the artificial chordae tendineae can be the first next steps to take. Fluid-structure interaction simulations, in order to evaluate the resulting stress on the leaflets and the stent, should be performed. Designing

a more realistic prototype with a nitinol stent and pericardial valve leaflets can also be suggested as a future work. In addition, there should be a mechanism developed for the purpose of anchoring the valve on the mitral valve annulus. Last but not least, it should be noticed that since the majority of prosthetic mitral valves have circular annuli, the laboratory facilities for testing the designed valves have circular annuli as well, which is a limitation for testing designs with an oval/D-shaped annuli.

References

[1] A. C. Guyton and J. E. Hall, *Guyton and Hall textbook of medical physiology e-Book*. Elsevier Health Sciences, 2015.

[2] "Circulatory System Organs and Their Functions." [Online]. Available: https://bodytomy.com/circulatory-system-organs.

[3] "Anatomy and Physiology," *ALGONQUIN College.* 2012. [Online]. Available: http://lyceum.algonquincollege.com/lts/onlineCourses/anatomy/content/module11-3.htm.

[4] L. Waite and J. Fine, "Applied Biofluid Mechanics," *Appl. biofluid Mech.*, p. 314p., 2007.

[5] P. Tips, "Anatomy and Physiology of the Heart," 2013. [Online]. Available: http://www.pharmatips.in/Articles/Human-Anatomy/Anatomy-Physiology-Of-The-Heart.aspx.

[6] M. Di Mauro *et al.*, "Functional mitral regurgitation: From normal to pathological anatomy of mitral valve," *Int. J. Cardiol.*, vol. 163, no. 3, pp. 242–248, 2013.

[7] J. K. Perloff and W. C. Roberts, "The Mitral Apparatus Functional Anatomy of Mitral Regurgitation," *Circulation*, vol. 46, pp. 227–239, 1972.

[8] S. Kaul, "The extents of mitral leaflet opening and closure are determined by left ventricular systolic function," *Heart*, vol. 90, no. 2, pp. 126–128, 2004.

[9] D. G. Reuter and P. M. Sullivan, "Translational Platform for Mitral Valve Repair and Replacement," *International Society for Cardiovascular Translational Research*, 2018. [Online]. Available: https://isctr.org/index.php/chapter-ii-7/.

[10] K. P. McCarthy, L. Ring and B. S. Rana, "Anatomy of the mitral valve: Understanding the mitral valve complex in mitral regurgitation," *Eur. J. Echocardiogr.*, vol. 11, no. 10, pp. 3–9, 2010.

[11] S. R. Kaplan *et al.*, "Three-dimensional echocardiographic assessment of annular shape changes in the normal and regurgitant mitral valve," *Am. Heart J.*, vol. 139, no. 3, pp.

378–387, 2000.

[12] H. Muresian, “The clinical anatomy of the mitral valve,” *Clin. Anat. Off. J. Am. Assoc. Clin. Anat. Br. Assoc. Clin. Anat.*, vol. 22, no. 1, pp. 85–98, 2009.

[13] “Mitral valve prolapse.” *MAYO Clinic.* [Online]. Available: https://www.mayoclinic.org/diseases-conditions/mitral-valve-prolapse/symptoms-causes/syc-20355446.

[14] J. Schmitto *et al.*, “Functional Mitral Regurgitation,” *Cardiol. Rev.*, vol. 18, no. 6, pp. 285–291, 2010.

[15] B. Heart and J. Steuter, “Mitraclip: A Minimally Invasive Procedure to Reduce Mitral Regurgitation,” *Bryan Health*. [Online]. Available: https://www.bryanhealth.com/medical-providers/the-beat-a-bryan-heart-blog/mitraclip/.

[16] D. Espiritu *et al.,* “Transcatheter Mitral Valve Repair Therapies: Evolution, Status and Challenges,” *Ann. Biomed. Eng.*, vol. 45, no. 2, pp. 332–359, 2017.

[17] S. Pant and K. J. Grubb, “Percutaneous Mitral Valve Technology: What Is on the Horizon?,” *Semin. Thorac. Cardiovasc. Surg.*, vol. 29, no. 4, pp. 447–450, 2017.

[18] F. Grigioni *et al.*, “Atrial fibrillation complicating the course of degenerative mitral regurgitation: determinants and long-term outcome,” *J. Am. Coll. Cardiol.*, vol. 40, no. 1, pp. 84–92, 2002.

[19] A. Barbieri *et al.*, “Prognostic and therapeutic implications of pulmonary hypertension complicating degenerative mitral regurgitation due to flail leaflet: a multicenter long-term international study,” *Eur. Heart J.*, vol. 32, no. 6, pp. 751–759, 2010.

[20] A. Hasudungan, “Mitral Regurgitaion (Insufficiency).” [Online]. Available: https://www.youtube.com/watch?v=uQ8Hz_c3bd4.

[21] “Mitral Vlave Disease (regurgitation, stenosis) - causes, symptoms and pathology,” *Osmosis*. 2016. [Online]. Available: https://www.youtube.com/watch?v=nY4aaBezu9o.

[22] “Mitral Valve Regurgitation,” *MAYO Clinic*. [Online]. Available:

https://www.mayoclinic.org/diseases-conditions/mitral-valve-regurgitation/diagnosis-treatment/drc-20350183.

[23] M. K. Rausch *et al.,* "Mitral valve annuloplasty: A quantitative clinical and mechanical comparison of different annuloplasty devices," *Ann. Biomed. Eng.*, vol. 40, no. 3, pp. 750–761, 2012.

[24] "Annuloplasty," *MAYO Clinic*. [Online]. Available: https://www.mayoclinic.org/tests-procedures/mitral-valve-repair-mitral-valve-replacement/multimedia/img-20302963.

[25] T. Holubec *et al.,* "Chordae replacement versus leaflet resection in minimally invasive mitral valve repair," *Ann. Cardiothorac. Surg.*, vol. 2, no. 6, p. 809, 2013.

[26] N. Kon and R. Riley, "Mitral Valve Repair," *CTSNet*, 2011. [Online]. Available: https://www.ctsnet.org/article/mitral-valve-repair.

[27] K. J. Park *et al.,* "Outcomes of mitral valve repair: quadrangular resection versus chordal replacement," *Korean J. Thorac. Cardiovasc. Surg.*, vol. 46, no. 2, p. 124, 2013.

[28] L. Salvador *et al.*, "A 20-year experience with mitral valve repair with artificial chordae in 608 patients," *J. Thorac. Cardiovasc. Surg.*, vol. 135, no. 6, pp. 1280–1288, 2008.

[29] X. Zhu *et al.,* "Echocardiographic assessment of long-term hemodynamic characteristics of mechanical mitral valve prostheses with different mitral valvular diseases," *Australas. Phys. Eng. Sci. Med.*, vol. 40, no. 1, pp. 259–266, 2017.

[30] "Mitral Valve Surgery," *Loyola Univercity Medical Center*. [Online]. Available: http://loyolamedicine.adam.com/content.aspx?productId=117&isArticleLink=false&pid=1&gid=007412.

[31] G. Hoffmann, G. Lutter and J. Cremer, "Durability of bioprosthetic cardiac valves," *Dtsch. Arztebl. Int.*, vol. 105, no. 8, p. 143, 2008.

[32] J. P. Mathew, M. Swaminathan and C. M. Ayoub, *Clinical Manual and Review of Transesophageal Echocardiography*, Second edi. .

[33] A. Kheradvar *et al.*, "Emerging Trends in Heart Valve Engineering: Part III. Novel

Technologies for Mitral Valve Repair and Replacement," *Ann. Biomed. Eng.*, vol. 43, no. 4, pp. 858–870, 2015.

[34] "Medtronic Hancock II," *MEDOL, Medical Online Services*. [Online]. Available: http://www.medol.uz/en/products/cardiac-surgery/heart-valves/medtronic-hancock-ii.html.

[35] J. Chikwe and F. Filsoufi, "Bioprosthetic Valves." [Online]. Available: http://www.themitralvalve.org/mitralvalve/types-of-bioprosthetic-valve.

[36] R. Violini *et al.*, "Treatment of mitral regurgitation," *Monaldi Arch. Chest Dis.*, vol. 87, no. 2, 2017.

[37] R. R. Jeevan and B. M. Murari, "Engineering challenges and the future prospects of transcatheter mitral valve replacement technologies: a comprehensive review of case studies," *Expert Rev. Med. Devices*, vol. 14, no. 4, pp. 297–307, 2017.

[38] P. T. L. Chiam and C. E. Ruiz, "Percutaneous transcatheter mitral valve repair," *JACC Cardiovasc. Interv.*, vol. 4, no. 1, pp. 1–13, 2011.

[39] B. Ramlawi and J. S. Gammie, "Mitral valve surgery: current minimally invasive and transcatheter options," *Methodist Debakey Cardiovasc. J.*, vol. 12, no. 1, p. 20, 2016.

[40] M. E. Guerrero *et al.*, "Transcatheter mitral valve replacement therapies," *Am. Coll. Cardiol. Expert Anal.*, 2017.

[41] A. Regueiro and J. Rodés-Cabau, "Percutaneous Mitral Valve Replacement, An overview of the transcatheter valve replacement therapies for treating mitral regurgitation," *Card. Interv. Today*, vol. 10, no. 4, pp. 44–48, 2016.

[42] O. A. J. Altisent *et al.*, "Initial experience of transcatheter mitral valve replacement with a novel transcatheter mitral valve: procedural and 6-month follow-up results," *J. Am. Coll. Cardiol.*, vol. 66, no. 9, pp. 1011–1019, 2015.

[43] S. Bozkurt *et al.*, "Design, Analysis and Testing of a Novel Mitral Valve for Transcatheter Implantation," *Ann. Biomed. Eng.*, vol. 45, no. 8, pp. 1852–1864, 2017.

[44] S. Farid *et al.*, "Early Outcomes After Mitral Valve Repair vs. Replacement in the Elderly:

A Propensity Matched Analysis," *Hear. Lung Circ.*, pp. 1–6, 2017.

[45] V. H. Thourani *et al.*, "Outcomes and long-term survival for patients undergoing mitral valve repair versus replacement: Effect of age and concomitant coronary artery bypass grafting," *Circulation*, vol. 108, no. 3, pp. 298–304, 2003.

[46] H. C. Herrmann and F. Maisano, "Transcatheter therapy of mitral regurgitation," *Circulation*, vol. 130, no. 19, pp. 1712–1722, 2014.

[47] M. J. King, T. David and J. Fisher, "An initial parametric study on fluid flow through bileaflet mechanical heart valves using computational fluid dynamics," *Proc lnstn Mech Engrs*, vol. 208, p. 63, 1994.

[48] A. M. Benson *et al.*, "Synthesis of a low thrombogenic heart valve coating with horseradish peroxidase," *Polym. Adv. Technol.*, vol. 16, no. 2–3, pp. 117–122, 2005.

[49] S. A. Reisner *et al.*, "Hemodynamic performance of four mechanical bileaflet prosthetic valves in the mitral position: An echocardiographic study," *Eur. J. Ultrasound*, vol. 8, no. 3, pp. 193–200, 1998.

[50] M. A. Marchand *et al.*, "Fifteen-year experience with the mitral Carpentier-Edwards PERIMOUNT Pericardial Bioprosthesis," *Ann. Thorac. Surg.*, vol. 71, no. 01, pp. S236–S239, 2001.

[51] C. M. Cunanan *et al.*, "Tissue Characterization and Calcification Potential of Commercial Bioprosthetic Heart Valves Drs Rutledge and Fishbein are paid consultants of," *Ann Thorac Surg*, vol. 71, pp. S417-21, 2001.

[52] C. Valfrè *et al.*, "The fate of Hancock II porcine valve recipients 25 years after implant," *Eur. J. Cardio-thoracic Surg.*, vol. 38, no. 2, pp. 141–146, 2010.

[53] S. Banai *et al.*, "Transapical mitral implantation of the tiara bioprosthesis: Pre-clinical results," *JACC Cardiovasc. Interv.*, vol. 7, no. 2, pp. 154–162, 2014.

[54] J. W. Hansen, G. Gadey and T. C. Piemonte, "Prosthetic mitral valve paravalvular leak: A problem that requires dexterity," *Cardiovasc. Revascularization Med.*, vol. 19, no. 1, pp. 126–132, 2018.

[55] S. Kumar *et al.*, "Minimally invasive left thoracotomy and prosthetic valve mini skirt for recurrent mitral paravalvular regurgitation," *Cor Vasa*, vol. 59, no. 5, pp. e477–e480, 2017.

[56] V. Stanova *et al.*, "Effect Of Valve Oversizing On Leaflet Bending Stress In The Corevalve: An In Vitro Study," *J. Am. Coll. Cardiol.*, vol. 69, no. 11 Supplement, p. 1044, 2017.

[57] A. W. Leber *et al.*, "MSCT guided sizing of the Edwards Sapien XT TAVI device: impact of different degrees of oversizing on clinical outcome," *Int. J. Cardiol.*, vol. 168, no. 3, pp. 2658–2664, 2013.

[58] F. Sotiropoulos, T. B. Le and A. Gilmanov, "Fluid mechanics of heart valves and their replacements," *Annu. Rev. Fluid Mech.*, vol. 48, pp. 259–283, 2016.

[59] R. Faludi *et al.*, "Left ventricular flow patterns in healthy subjects and patients with prosthetic mitral valves: an in vivo study using echocardiographic particle image velocimetry," *J. Thorac. Cardiovasc. Surg.*, vol. 139, no. 6, pp. 1501–1510, 2010.

[60] M. Gharib *et al.*, "Optimal vortex formation as an index of cardiac health," *Proc. Natl. Acad. Sci.*, vol. 103, no. 16, pp. 6305–6308, 2006.

[61] E. Ghosh and S. J. Kovács, "E-Wave Associated Vortex Formation Facilitates Diastatic Mitral Leaflet Coaptation," *J. Am. Coll. Cardiol.*, vol. 57, no. 14, p. E663, 2011.

[62] G. Pedrizzetti, F. Domenichini and G. Tonti, "On the left ventricular vortex reversal after mitral valve replacement," *Ann. Biomed. Eng.*, vol. 38, no. 3, pp. 769–773, 2010.

[63] K. D. Lau, *et al.*, "Mitral valve dynamics in structural and fluid–structure interaction models," *Med. Eng. Phys.*, vol. 32, no. 9, pp. 1057–1064, 2010.

[64] H. Reul, N. Talukder and E. W. Mu, "Fluid mechanics of the natural mitral valve," *J. Biomech.*, vol. 14, no. 5, pp. 361–372, 1981.

[65] "3D HUBS." [Online]. Available: https://www.3dhubs.com/knowledge-base/pla-vs-abs-whats-difference.

[66] "XIAMETER® RTV-4234-T4 Base and XIAMETER® T4/T4 O Curing Agent." [Online]. Available: http://mbfgfiles.co.uk/datasheets/t4_tech.pdf.

[67] M. O. Karlsson *et al.*, "Mitral valve opening in the ovine heart.," *Am. J. Physiol.*, vol. 274, no. 2 Pt 2, pp. H552-63, 1998.

[68] A. Goharzadeh and A. Molki, "Measurement of fluid velocity development behind a circular cylinder using particle image velocimetry (PIV)," *Eur. J. Phys.*, vol. 36, no. 1, p. 15001, 2014.

[69] D. Dabiri, "Cross-Correlation Digital Particle Image Velocimetry-A Review," *Dep. Aeronaut. Astronaut. Box 352400 Univ. Washingt.*, pp. 1–54, 2006.

[70] M. Jeyhani, "Left Ventricular Flow Patterns after Percutaneous Edge-to-Edge Mitral Valve Repair: An in vitro Study," Concordia University, 2013.

[71] B. H. Timmins *et al.*, "A method for automatic estimation of instantaneous local uncertainty in particle image velocimetry measurements," *Exp. Fluids*, vol. 53, no. 4, pp. 1133–1147, 2012.

[72] M. Raffel *et al.*, *Particle Image Velocimetry Guide*, Second Edition. Springer, 2007.

[73] S. Nishio, "Uncertainty Analysis: Particle Imaging Velocimetry (PIV)," *ITTC – Recomm. Proced. Guidel.*, 2008.

[74] L. Graftieaux, M. Michard and N. Grosjean, "Combining PIV, POD and Vortex Identification Algorithms for the Study of Unsteady Turbulent Swirling Fows," vol. 12, pp. 1422–1429, 2001.

[75] T. Günther and H. Theisel, "The State of the Art in Vortex Extraction," *Comput. Graph. Forum*, vol. 37, no. 6, pp. 149–173, 2018.